Development of Covalent Ligands for G Protein-Coupled Receptors: A Case for the Human Adenosine A3 Receptor

Yang, X.; Veldhoven, J.P.D. van; Offringa, J.; Kuiper, B.J.; Lenselink, E.B.; Heitman, L.H.; ... ; IJzerman, A.P.

Journal of Medicinal Chemistry

Article

Cite This: J. Med. Chem. 2019, 62, 3539−3552

pubs.acs.org/jmc

Development of Covalent Ligands for G Protein-Coupled Receptors: A Case for the Human Adenosine A_3 Receptor

Xue Yang, Jacobus P. D. van Veldhoven, Jelle Offringa, Boaz J. Kuiper, Eelke B. Lenselink, Laura H. Heitman, Daan van der Es, and Adriaan P. IJzerman*

Division of Drug Discovery and Safety, Leiden Academic Centre for Drug Research, Leiden University, Einsteinweg 55, 2333 CC Leiden, The Netherlands

Supporting Information

ABSTRACT: The development of covalent ligands for G protein-coupled receptors (GPCRs) is not a trivial process. Here, we report a streamlined workflow thereto from synthesis to validation, exemplified by the discovery of a covalent antagonist for the human adenosine A_3 receptor (hA_3AR). Based on the 1*H*,3*H*-pyrido[2,1-*f*]purine-2,4-dione scaffold, a series of ligands bearing a fluorosulfonyl warhead and a varying linker was synthesized. This series was subjected to an affinity screen, revealing compound **17b** as the most potent antagonist. In addition, a nonreactive methylsulfonyl derivative **19** was developed as a reversible control compound. A series of assays, comprising time-dependent affinity determination, washout experiments, and [^{35}S]GTPγS binding assays, then validated **17b** as the covalent antagonist. A combined in silico hA_3AR-homology model and site-directed mutagenesis study was performed to demonstrate that amino acid residue Y265$^{7.36}$ was the unique anchor point of the covalent interaction. This workflow might be applied to other GPCRs to guide the discovery of covalent ligands.

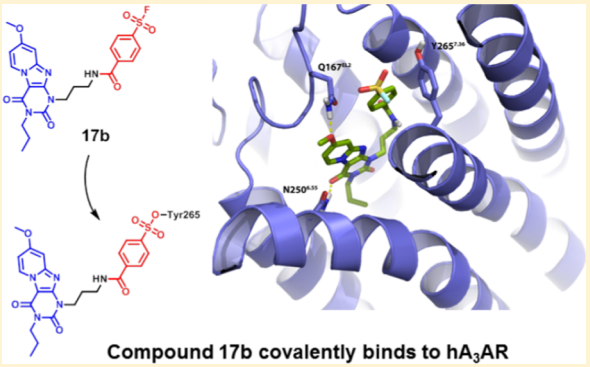

INTRODUCTION

The adenosine A_3 receptor (A_3AR) is one of four G protein-coupled receptor subtypes stimulated by adenosine.[1] Different from the other subtypes (A_1, A_{2A}, and A_{2B}) A_3AR was identified by molecular biology studies prior to its pharmacological characterization.[2] The initial studies indicated its important role in both physiological and pathophysiological conditions, such as cell proliferation, cell differentiation, neuroprotection, cardioprotection, and apoptosis.[3] Nevertheless, the medical relevance of the human adenosine A_3 receptor (hA_3AR) is enigmatic due to its dichotomy in different therapeutic applications.[3] In this regard, there is a continuing interest in the development of selective ligands of the hA_3AR to investigate its pharmacological effects. For instance, selective A_3AR antagonists have been applied for the treatment of glaucoma[4] and respiratory tract inflammation such as asthma.[5] In particular, a tricyclic xanthine derivative, 1-benzyl-8-methoxy-3-propyl-1*H*,3*H*-pyrido[2,1-*f*]purine-2,4-dione (compound **1**, Figure 1A), has been reported to exert high affinity for the hA_3AR.[6−8]

Initial efforts to study the structural biology of GPCRs suffered from numerous limitations, such as low expression, dynamic conformational states, and inherent instability. Covalent ligands, i.e., compounds that irreversibly bind to the receptor and possess a reactive moiety to target specific amino acid residues, helped to solve some of these obstacles.[9] This is also the case for adenosine receptors. For example, the

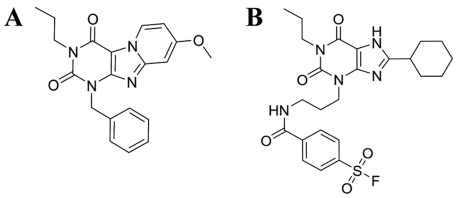

Figure 1. (A) Reference antagonist (**1**) for hA_3AR. (B) DU172 (**2**), a covalent antagonist for hA_1AR.

structure of the human adenosine A_1 receptor, having the highest similarity to the hA_3AR among all adenosine receptor subtypes (61% of sequence homology),[10] has been elucidated by X-ray crystallography with a covalent antagonist DU172 (**2**) (Figure 1B).[11] However, the application of covalent ligands in hA_3AR studies has been limited to the characterization of the receptor type,[12−14] far from providing a comprehensive study of receptor structure elucidation, pharmacological characteristics, and ligand−receptor binding description.

To this end, we devoted our efforts to the discovery of a well-defined covalent antagonist based on xanthine analogue **1** mentioned above. Inspired by the resemblance in the chemical

Received: December 27, 2018
Published: March 14, 2019

DOI: 10.1021/acs.jmedchem.8b02026
J. Med. Chem. 2019, 62, 3539−3552

Scheme 1. Synthetic Route toward Scaffold 7[a]

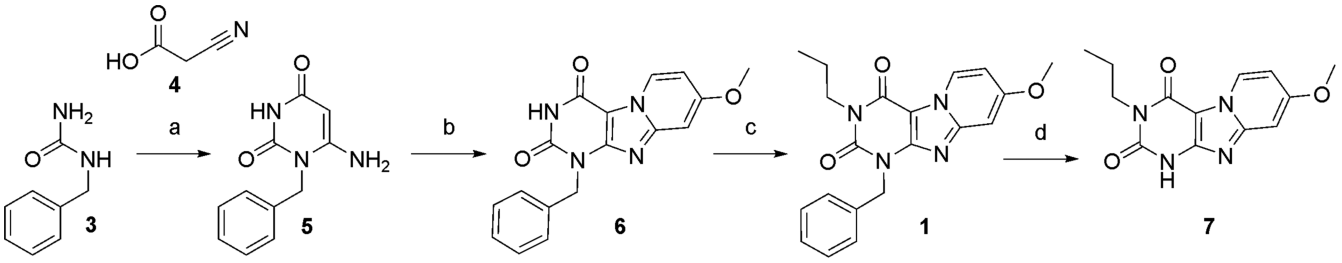

[a]Reagents and conditions: (a) (i) Ac_2O, 80 °C, 2 h; (ii) Et_2O, room temperature (rt), 1 h; (iii) 3 M NaOH, 85 °C, 1 h; (iv) HCl (37%), 25%; (b) (i) NBS, MeCN, 80 °C; (ii) 4-methoxypyridine, 80 °C, 64%; (c) 1-bromopropane, 1,8-diazabicyclo[5.4.0]undec-7-ene (DBU), MeCN, 70 °C, 73%; (d) $Pd(OH)_2/C$, $HCOONH_4$, EtOH, reflux, 40%.

Scheme 2. Synthetic Route toward the Bromoalkyl Fluorosulfonylbenzoates 13a−c and 14a−c[a]

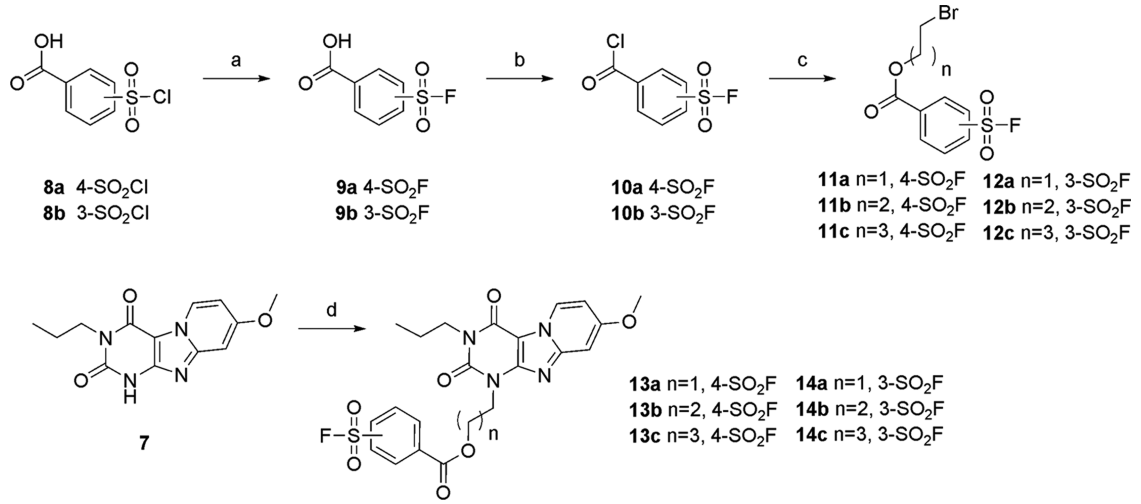

[a]Reagents and conditions: (a) 2 M KHF_2 solution, dioxane, rt, 1 h, 87−90%; (b) $SOCl_2$ reflux; (c) corresponding bromoalkylalcohol, anhydrous dioxane, 100 °C, 18h, 55−83%, (d) **11a−c** or **12a−c**, K_2CO_3, anhydrous DMF, 50 °C, 5−57%.

structure between the potent hA_3AR antagonist **1** and irreversible adenosine A_1 receptor antagonist **2**, we incorporated the reactive moiety, a fluorosulfonyl benzoyl group, connected to a spacer, at the N^1 position of the scaffold. Using a structured approach to bring the reactive fluorosulfonyl group in close proximity to a nucleophilic amino acid residue, we diversified the type of linker, linker length, and position of the fluorosulfonyl substituent on the phenyl group, resulting in a series of analogues with a wide range of affinities. Our efforts led to the discovery of a best-in-class antagonist, **17b**, which is bound to the hA_3AR with an apparent affinity in the nanomolar range. To retain the chemical structure similarity, we replaced the warhead with a methylsulfonyl moiety to obtain a nonreactive derivative **19** as a reversible control compound. **17b** was then validated to covalently bind and inactivate the hA_3AR in an insurmountable manner. Molecular modeling suggested the fluorosulfonyl functionality of **17b** in close proximity to $Y265^{7.36}$, which was identified as the unique anchor point of the covalent interaction in a subsequent mutagenesis study. The confirmed binding mode between this novel covalent antagonist and hA_3AR opens the door for exploring other ligand binding motifs and will benefit receptor stabilization and further structure elucidation of the hA_3AR.

RESULTS AND DISCUSSION

Design of Covalent hA_3AR Antagonists. In previous studies, our research group disclosed several series of hA_3AR antagonists based on the pyrido[2,1-*f*]purine-2,4-dione scaffold.[6−8] Using compound **1**, a nanomolar probe from the previous series, as the starting point, we further designed and synthesized compounds based on a previously suggested binding mode of the pyrido[2,1-*f*]purine-2,4-dione scaffold.[7] When examining the suggested binding mode of this scaffold, we noted that this scaffold inserted into the binding pocket with a receptor interaction between TM3, TM6, and EL2. Two key H-bonds include the carbonyl-oxygen at the C^4-position with residue $N250^{6.55}$ and the methoxy substituent at the C^8-position bonding to $Q167^{EL2}$. Taking this into account, we reasoned that the only available space to incorporate the reactive warhead is limited to N^1-position substituents.

To explore the chemical space required to optimally position the warhead in close proximity to a nucleophilic amino acid residue, we examined various linker systems, connecting the warhead and the pyrido[2,1-*f*]purine-2,4-dione scaffold. First, variation in the length of the spacer, between two and four carbon atoms, may offer more steric freedom allowing the fluorosulfonyl group to orient toward an adjacent nucleophilic residue in the receptor binding site.[15,16] Additionally, the type of chemical bond connecting the warhead to the spacer was varied between the slightly differently oriented ester or amide

DOI: 10.1021/acs.jmedchem.8b02026
J. Med. Chem. 2019, 62, 3539−3552

Scheme 3. Synthetic Route toward the Amide-Linker Antagonists 17a−c, 18a−c, and 19[a]

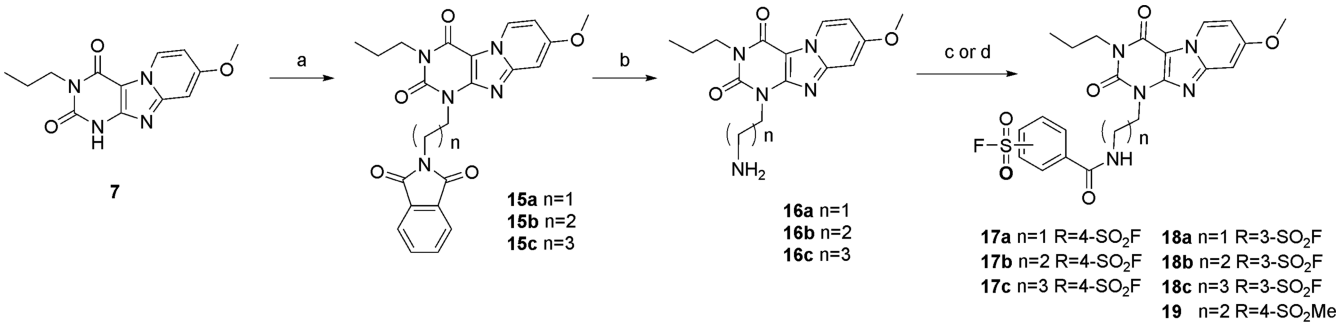

[a]Reagents and conditions: (a) *N*-(bromoalkyl)phthalimide, K_2CO_3, DMF, 100 °C, 5−96%; (b) $N_2H_4{\cdot}H_2O$, MeOH reflux, 86−90%; (c) 1-ethyl-3-(3-dimethylaminopropyl)carbodiimide (EDC), corresponding acid (**9a,b**), $CHCl_3$ or CH_2Cl_2, rt; and (d) $SOCl_2$, K_2CO_3, dry DMF, 40 °C, 3−78%

Table 1. Apparent Affinities of Pyrido[2,1-*f*]purine-2,4-dione Derivatives 13−19

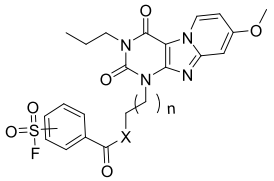

compound	*n*	X	R^1	$pK_i \pm SEM$[a] or disp. at 10 μm (%)
13a	1	O	4-SO_2F	6.7 ± 0.1
13b	2	O	4-SO_2F	7.7 ± 0.1
13c	3	O	4-SO_2F	7.5 ± 0.1
14a	1	O	3-SO_2F	6.4 ± 0.1
14b	2	O	3-SO_2F	7.0 ± 0.05
14c	3	O	3-SO_2F	7.1 ± 0.05
17a	1	NH	4-SO_2F	27%
17b (LUF7602)	2	NH	4-SO_2F	8.0 ± 0.05
17c	3	NH	4-SO_2F	7.5 ± 0.05
18a	1	NH	3-SO_2F	18%
18b	2	NH	3-SO_2F	7.5 ± 0.01
18c	3	NH	3-SO_2F	6.8 ± 0.1
19 (LUF7714)	2	NH	4-SO_2Me	6.3 ± 0.03

[a]Data are expressed as means ± standard error of the mean (SEM) of three separate experiments each performed in duplicate. Apparent affinity determined from the displacement of specific [^{3}H]PSB-11 binding from the hA_3AR stably expressed on Chinese hamster ovary (CHO) cell membranes at 25 °C during 2 h of incubation.

bond. Finally, since the exact position of an appropriate nucleophilic residue is unknown, the sulfonyl fluoride moiety was positioned at either the 3- or 4-position of the phenyl ring. To this end, four series of compounds **13a−c**, **14a−c**, **17a−c**, and **18a−c**, bearing three different spacer lengths, ester or amide linkage, and 3- or 4-fluorosulfonylphenyl warhead were targeted for synthesis.

Synthesis. *Scaffold.* The scaffold, 8-methoxy-3-propyl-1*H*,3*H*-pyrido-[2,1-*f*]purine-2, 4-dione (**1**), was synthesized according to the previously published procedure.[6−8] Starting from the commercially available benzylurea (**3**), the fused tricyclic intermediate (**6**) was generated by excess *N*-bromosuccinimide (NBS) bromination and 4-methoxypyridine cyclization (Scheme 1). Then, alkylation at the N^3-nitrogen by 1-bromopropane in dry dimethylformamide (DMF), using dry potassium carbonate as a weak base, afforded the reference compound (**1**) in 73% yield. Removing the benzyl protecting group by palladium hydroxide afforded the fused xanthine core (**7**).

Ester Linker. The fluorosulfonyl warhead is notorious for its reactivity, resulting in undesired side reactions or hydrolysis under several harsh reactions.[17] So, we adopted a convergent synthetic strategy in which the fluorosulfonylphenyl linker unit was prepared separately and attached directly to scaffold **7** at the N^3 position. This approach offers flexibility to accommodate a variety of different linker lengths. The warhead was synthesized from commercially available chlorosulfonylbenzoic acids (**8a** and **8b**) (Scheme 2), followed by a 2 M solution of potassium bifluoride treatment to afford fluorosulfonylbenzoic acids (**9a** and **9b**) in good yields.[18] The next step converted the carboxylic acids to acid chlorides (**10a** and **10b**) by excess thionyl chloride treatment. These acyl chlorides are susceptible to hydrolysis and were thus used in the next step reaction without further purification. To incorporate the acyl chlorides with the corresponding bromoalkylalcohols, compounds **10a** and **10b** were heated to 100 °C with the addition of bromoalkylalcohols to afford the desired bromoalkyl fluorosulfonylbenzoates (**11a−c** and **12a−c**) in decent yields. The final step was to couple the core to the corresponding bromoalkyl fluorosulfonylbenzoates. To preserve the functional fluorosulfonyl group, the reactions were carried out under mild conditions at low temperatures. Additionally,

DOI: 10.1021/acs.jmedchem.8b02026
J. Med. Chem. 2019, 62, 3539−3552

Table 2. (Apparent) Affinities of 17b and 19 for All Adenosine Receptor Subtypes, hA_3AR-WT, and hA_3AR-Y265F$^{7.36}$ [a]

	hA_1AR[b]	$hA_{2A}AR$[c]	$hA_{2B}AR$[d]	hA_3AR		hA_3AR-WT[g]	hA_3AR-Y265F$^{7.36}$ [h]
cpd	$pK_i \pm$ SEM		displ. (%) at 1 μm	pK_i[e] (pre-0 h)	pK_i[f] (pre-4 h)	$pIC_{50} \pm$ SEM[f]	
17b[i]	6.1 ± 0.03	5.9 ± 0.09	0% (7, −7)	6.9 ± 0.06	8.0 ± 0.01**	7.8 ± 0.05	6.0 ± 0.3*
19	4.8 ± 0.20	5.2 ± 0.20	0% (−10, −13)	6.2 ± 0.03	6.1 ± 0.06^{NS}	5.9 ± 0.02	6.1 ± 0.1^{NS}

[a]Values represent mean ± SEM of three separate experiments, each performed in duplicate, or percentage displacement at 1 μm of two separate experiments, each performed in duplicate. [b]Affinity determined from the displacement of specific [^{3}H]DPCPX binding on CHO cell membranes stably expressing human adenosine A_1 receptors at 25 °C during 2 h of incubation. [c]Affinity determined from the displacement of specific [^{3}H]ZM241385 binding on HEK293 cell membranes stably expressing human adenosine A_{2A} receptors at 25 °C during 2 h of incubation. [d]% displacement at 1 μm concentration of specific [^{3}H]PSB-603 binding on CHO cell membranes stably expressing human adenosine A_{2B} receptors at 25 °C during 2 h of incubation. [e]Displacement of specific [^{3}H]PSB-11 binding on CHO cell membranes stably expressing the hA_3AR at 25 °C during 0.5 h of incubation. [f]Displacement of specific [^{3}H]PSB-11 binding from CHO cell membranes stably expressing the hA_3AR preincubated with an antagonist for 4 h at 25 °C, followed by a 0.5 h of co-incubation with [^{3}H]PSB-11. $P < 0.01$** compared with the pK_i values in displacement experiments during 0.5 h of incubation time; NS: no significant difference compared with the pK_i values in displacement experiments during 0.5 h of incubation time; Student's test. [g]Displacement of specific [^{3}H]PSB-11 binding from CHO-K1 cell membranes transiently transfected with hA_3AR-WT at 25 °C during 2 h of incubation. [h]Displacement of specific [^{3}H]PSB-11 binding from CHO-K1 cell membranes transiently transfected with hA_3AR-Y265F$^{7.36}$ at 25 °C during 2 h of incubation. $P < 0.01$* compared with the pIC_{50} values in displacement experiments on hA_3AR-WT. NS: no significant difference compared with the pIC_{50} values in displacement experiments on hA_3AR-WT membranes; Student's test. [i]For **17b**, pK_i values are apparent affinity values as no dynamic equilibrium can be obtained.

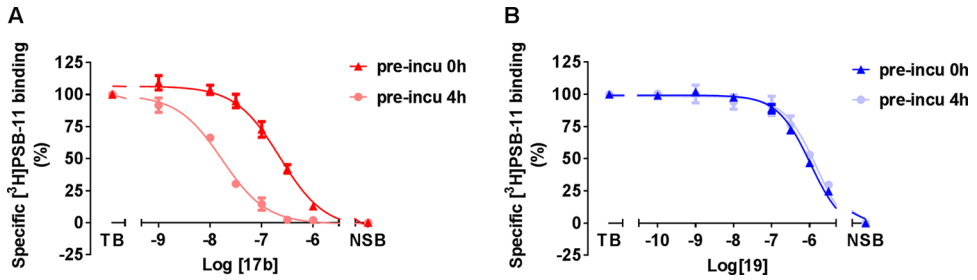

Figure 2. (A) Displacement of [^{3}H]PSB-11 binding from the hA_3AR at 25 °C by **17b** with and without preincubation of 4 h. (B) Displacement of [^{3}H]PSB-11 binding from the hA_3AR at 25 °C by **19** with and without preincubation of 4 h. Data represent the mean ± SEM of three individual experiments performed in duplicate.

excess DMF was removed by multiple washing steps, instead of vacuum removal at high temperatures. Six final products (**13a−c** and **14a−c**) were obtained in acceptable yields.

Amide Linker. A similar synthetic approach was initially pursued to prepare analogues with an amide linker. However, the basicity and instability of bromoalkylamine caused complex side reactions with itself and with the warhead, ending up with an unacceptably low yield of amide-linked building blocks. An alternative synthetic route was devised, where 1-phthalimidopropyl bromide was attached directly to the N^3 position of scaffold **6**, to afford the substituted intermediates **15a−c** (Scheme 3). Liberation of the amine took place by treatment with hydrazine monohydrate in methanol to obtain compound **16a−c** in moderate yield. Then **16b** and **16c** were acylated with acyl chlorides **10a** and **10b**, respectively, to obtain **17c** and **18b**. However, impurities brought by the acylation reaction were not easily removed by column chromatography or preparative thin-layer chromatography (TLC). To overcome this, we used peptide coupling conditions with the corresponding benzoic acids (**9a** and **9b**) to convert the free amine to the target compounds (**17a**,**b**, **18a**, and **18c**) in good yields (Scheme 3). A similar synthetic strategy was adapted to obtain reversible ligand **19** as a control compound.

Pharmacological Evaluation. *Determination of the Apparent Affinity (K_i) of Synthetized Ligands.* To determine the binding affinity for the hA_3AR, all compounds were tested in a radioligand displacement binding assay in the presence of 10 nM [^{3}H]PSB-11 at 25 °C according to previously reported procedures.[7,19] All compounds were able to concentration-dependently inhibit specific [^{3}H]PSB-11 binding to the hA_3AR. As detailed in Table 1, all putative covalent compounds, except the two carbon linker compounds (**13a**, **14a**, **17a**, and **18a**), displayed high affinities for the hA_3AR (K_i < 100 nM). It should be mentioned that the putative covalent nature of the interaction between the hA_3AR and ligands precludes the determination of equilibrium binding parameters. Therefore, we expressed the ligands' affinity for the hA_3AR as "apparent K_i". Of note, **17b**, bearing three carbon atoms with amide linkage and positioning the sulfonyl fluoride at the 4-position of the phenyl ring, interacted with the hA_3AR with comparable affinity (10 nM) as the parent compound **1**. High affinity is desirable for covalent ligand design, as it allows sufficient receptor occupancy with the electrophilic warhead in proximity to a nucleophilic residue in the binding site over time, concomitant with putatively negligible or less interaction with off-targets. Thus, we chose compound **17b** for further studies. However, featuring an electrophilic fluorosulfonyl functionality, **17b** was no longer a close analogue of compound **1**, whereas a nonreactive control compound, chemically similar to the designed covalent ligand, is needed for the further pharmacological characterization.

A nonsubstituted phenyl to replace the warhead might impose different steric and electronic characteristics of the ligand. To avoid this, we performed a conservative structural modification to replace the reactive warhead with an electron-withdrawing methylsulfonyl group, yielding derivative **19** as a nonreactive control compound.

DOI: 10.1021/acs.jmedchem.8b02026
J. Med. Chem. 2019, 62, 3539−3552

To better understand the time-dependent binding characteristics of these compounds, we carried out radioligand displacement assays under two different protocols. In detail, the CHO cell membranes overexpressing the hA_3AR were either preincubated with the indicated compound for 4 h, followed by a 0.5 h co-incubation or only co-incubated for 0.5 h with the radioligand [^{3}H]PSB-11. As detailed in Table 2, both compounds had comparable binding affinity in the low micromolar range ($pK_i = 6.9 \pm 0.06$ for **17b** and $pK_i = 6.2 \pm 0.03$ for **19**) at 0.5 h incubation time. However, compound **17b** showed a significantly increased affinity ($pK_i = 8.0 \pm 0.01$) when it was preincubated with the hA_3AR, whereas the affinity of compound **19** did not change ($pK_i = 6.1 \pm 0.06$). The effect of preincubation on the affinity of **17b** and **19** is illustrated in Figure 2, i.e., the [^{3}H]PSB-11 displacement curve was shifted to the left with an increased incubation time for compound **17b** (Figure 2A), whereas no difference was observed for compound **19** (Figure 2B).

Presumably, this time-dependent binding affinity of compound **17b** (i.e., resulting from an increased receptor occupancy over time) is a result of an increasing level of covalent binding. Similar results on other GPCRs, such as β_2 adrenergic receptor[20] and A_{2A} adenosine receptor,[21] showed that covalent bond formation generates an increased affinity over time. Meanwhile, control compound **19** showed no substantial pK_i shift in affinity at the two incubation times, indicating that a dynamic equilibrium was achieved at both incubation times. We can thus speculate that the possible covalent interaction between compound **17b** and the receptor may be attributed to the presence of a reactive warhead.

Finally, we tested **17b** and **19** for their affinity on the other adenosine receptor subtypes and learned that the two compounds were at least modestly selective for the hA_3AR (Table 2).

Kinetic Characterization of the Covalent Ligand. Subsequently, the significant shift in apparent K_i drove us to explore the binding kinetic profile of **17b** at the hA_3AR, specifically its dissociation rate and residence time (RT). Previously, the k_{on} ($k_1 = 0.281 \pm 0.04 \times 10^8$ M^{-1} min^{-1}) and k_{off} ($k_2 = 0.3992 \pm 0.02$ min^{-1}) values of [^{3}H]PSB-11 at 25 °C had been determined in our laboratory by traditional association and dissociation assays. Here, we performed a competition association assay to characterize the binding kinetics of **17b** and **19** following previously reported procedures from our research group.[7] Using the on- and off-rate constants from [^{3}H]PSB, the k_{on} (k_3) and k_{off} (k_4) values for **17b** were determined using the equations from the (equilibrium) Motulsky and Mahan model.[22] **17b** had a much slower association rate ($k_{on} = 3.48 \pm 0.22 \times 10^5$ M^{-1} min^{-1}) than the radioligand and a negligible dissociation rate ($k_{off} = 1.38 \pm 0.22 \times 10^{-12}$ min^{-1}), yielding an almost infinite residence time (RT = $7.63 \pm 1.19 \times 10^{11}$ min), indicative of irreversible receptor binding by **17b**. The inadequacy of the Motulsky–Mahan equations to fit this data is further evidence for the nonequilibrium features of the binding of **17b** to the receptor. Compound **19** showed fast association and dissociation rate constants (Figure 3). Unfortunately, the data did not converge in the fitting procedure, possibly due to the low binding affinity of compound **19** (K_i = 525 nM).

As detailed in Figure 3, the control curve represented the association curve of radioligand [^{3}H]PSB-11 alone, approaching equilibrium over time. Compound **19** equally associated with and dissociated from the receptor and reached

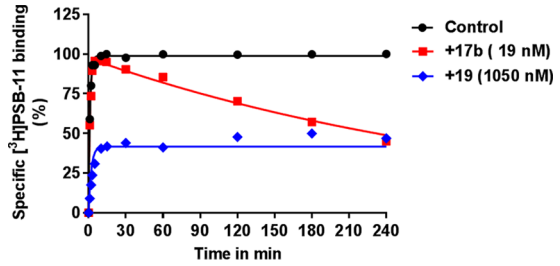

Figure 3. Competition association assay of [^{3}H]PSB-11 in the absence (control) or presence of **17b** and **19** at the indicated concentration. Association and dissociation rate constants for the unlabeled ligands were calculated by fitting the data to the equations described in the Experimental Section ("data analysis"). Representative graphs are from one experiment performed in duplicate.

equilibrium within 30 min, evidenced by the same curve shape as the control curve. Of note, **17b**'s behavior caused an initial "overshoot" of the competition association curve, followed by a linear decline over time indicating that no equilibrium was reached. The shape of **17b**'s kinetic curve is a quintessential example for the irreversible interaction, similar to the reported covalent ligands' behavior for the adenosine A_{2A} receptor[21] and mGlu2 receptor.[23]

*Wash-Resistant Interaction between **17b** and hA_3AR.* Inspired by the negligible dissociation of compound **17b** from the hA_3AR, we performed a "washout" experiment to ascertain the irreversible binding between the ligand and the receptor. A protocol previously reported by our laboratory[21] was adapted. We first exposed hA_3AR cell membranes to **17b** or **19** both at 10-fold K_i for 2 h, and without washing the samples were supplemented with [^{3}H]PSB-11 to assess the competitive binding capacity of the receptor ("control group" in Figure 4).

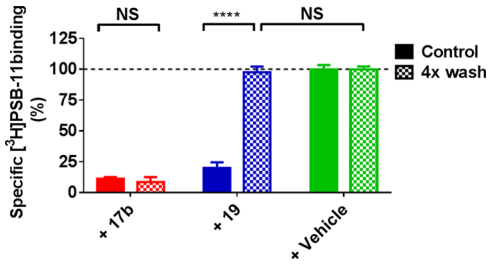

Figure 4. hA_3AR membranes preincubated with buffer (vehicle) or a $10 \times K_i$ concentration of indicated ligand, followed by no washing (control) or four-cycle washing treatment (4× wash) before being exposed to [^{3}H]PSB-11. Data represent the mean ± SEM of three individual experiments performed in duplicate, normalized to the vehicle (set at 100%). Statistics were determined using unpaired Student's *t*-test. NS: no significant difference, ****$P < 0.0001$, significant difference between indicated groups.

For washed samples, hA_3AR cell membranes were subjected to four-cycle washing steps to remove unbound ligand following the preincubation ("4× wash group" in Figure 4), after which the membranes were exposed to [^{3}H]PSB-11 to determine the remaining binding capacity. In the absence of the ligand (labeled "+ vehicle" in Figure 4), we normalized membranes' binding ability to 100%. Following preincubation with **17b**, membranes containing the hA_3AR lost most of the ability to bind to the radioligand (11.3 ± 1.2% binding remaining). Furthermore, after the preincubation, membranes were washed by cycles of centrifugation in an attempt to regenerate binding

DOI: 10.1021/acs.jmedchem.8b02026
J. Med. Chem. 2019, 62, 3539−3552

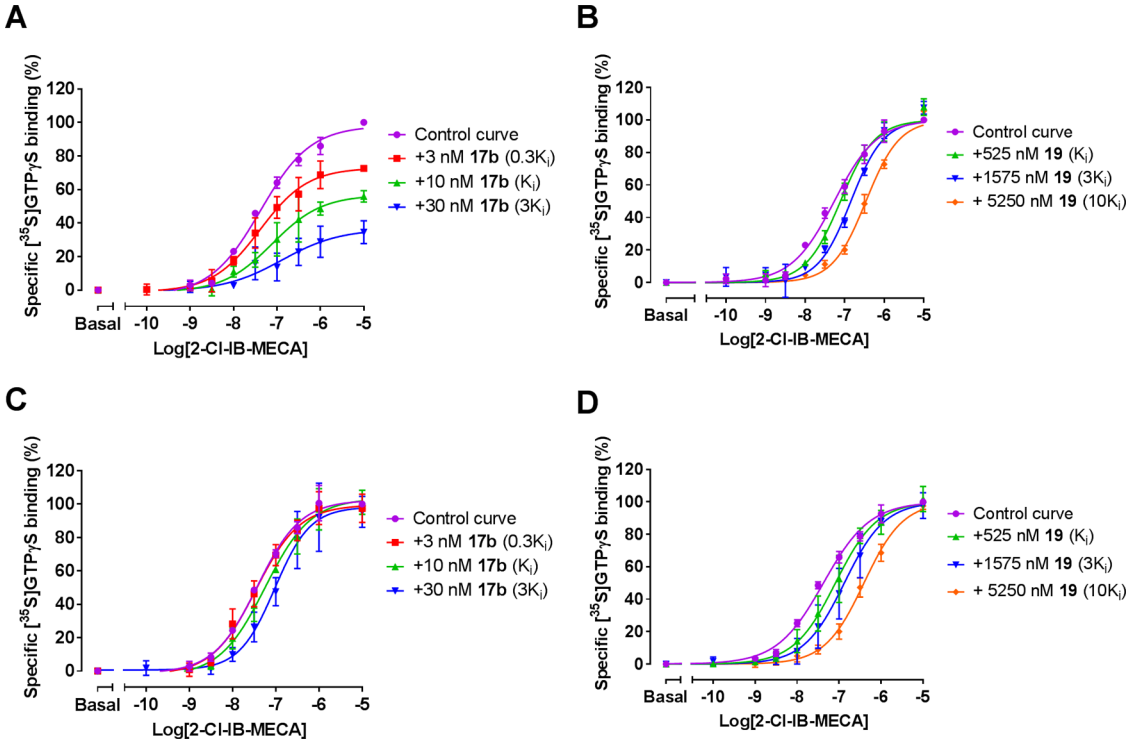

Figure 5. Effects of **17b** and **19** on hA_3AR activation as measured by [^{35}S]GTPγS binding. (A, B) Compound **17b** (A) or **19** (B) was preincubated with the hA_3AR stably expressed on CHO cell membranes (25 °C) for 60 min prior to the addition of 2-Cl-IB-MECA at a concentration ranging from 0.1 nM to 10 μm for 30 min. (C, D) Compound **17b** (C) or **19** (D) were co-incubated with 2-Cl-IB-MECA, at a concentration ranging from 0.1 nM to 10 μm, for 30 min. The agonist curves were generated in the presence of increasing concentrations of antagonists, such as 0.3-, 1-, 3-, and 10-fold K_i values, respectively. Data are from three independent experiments performed in duplicate, normalized according to the maximal response (100%) produced by 10 μm 2-Cl-IB-MECA alone. The shift in agonist EC_{50} values was determined to perform Schild analyses.

Table 3. Functional Analysis of hA_3AR Antagonism from [^{35}S]GTPγS Binding Assays[a]

	preincubation		co-incubation		
compound	pA_2	Schild slope	pA_2	Schild slope	mode of antagonism
17b	NA	NA	7.4 ± 0.1	1.1 ± 0.1	competitive insurmountable
19	5.9 ± 0.1	1.1 ± 0.1	6.2 ± 0.1	1.0 ± 0.1	competitive surmountable

[a]Values represent mean ± SEM of three separate experiments each performed in duplicate.

capacity. However, washing steps failed to restore hA_3AR binding of [^{3}H]PSB-11 (8.7 ± 3.8%). This was in contrast to preincubation of the hA_3AR-expressing membranes with ligand **19**, in which binding function was completely restored from 19.8 ± 4.7 to 97.6 ± 4.5% following four washing steps. This result indicates that **19** is a reversible ligand which can be rapidly washed off the membranes, whereas **17b** forms a wash-resistant bond between the ligand and the receptor. Similar experiments on other GPCRs, such as adenosine A_1[24,25] and A_{2A}[21] receptors and the metabotropic glutamate receptor 2 (mGluR2),[23] demonstrated that the covalent interaction between the ligand and the receptor resulted in a wash-resistant bond formation.

Insurmountable Antagonism Caused by Covalent Interaction. To further evaluate the effect of irreversible inhibition by covalent ligand **17b** on receptor function, we performed a membrane functional assay using [^{35}S]GTPγS, which is a typical readout for the activation of receptor-coupled $G_{i/o}$ proteins.[26] Pretreatment of the hA_3AR with increasing concentrations of ligand **17b**, prior to the stimulation with hA_3AR agonist 1-[2-chloro-6-[[(3-iodophenyl)methyl]amino]-9*H*-purin-9-yl]-1-deoxy-*N*-methyl-β-D-ribofuranuronamide (2-Cl-IB-MECA), produced rightward shifts of agonist concentration−response curves with a concomitant decline in maximal stimulation (Figure 5A). Therefore, the covalent ligand **17b** generated insurmountable antagonism in the preincubation experiment. In contrast, pretreatment of the hA_3AR with **19**, followed by 2-Cl-IB-MECA agonist exposure resulted in surmountable antagonism (Figure 5B), i.e., shifting dose−response curves to the right with no alteration of its maximum effect. The extent of the shifts was used to construct a Schild plot as previously described,[7] which would have a slope of unity if the interaction is competitive and the pA_2-value corresponds to the pK_i value of the antagonist. The slope for **19** was found to be 1.1 ± 0.1 and the compound's pA_2 value was 5.9 ± 0.1, comparable with its pK_i value (6.3 ± 0.03), suggesting that **19** competed with 2-Cl-IB-MECA for the same receptor binding site.

To unravel the molecular mechanism responsible for the insurmountable antagonism of **17b**, we also co-incubated either **17b** or **19** with the hA_3AR in the presence of 2-Cl-IB-MECA. Both ligands produced a rightward shift of the agonist's concentration−response curve (Figure 5C,D) with no suppression of maximal response, indicative of surmountable

DOI: 10.1021/acs.jmedchem.8b02026
J. Med. Chem. 2019, 62, 3539−3552

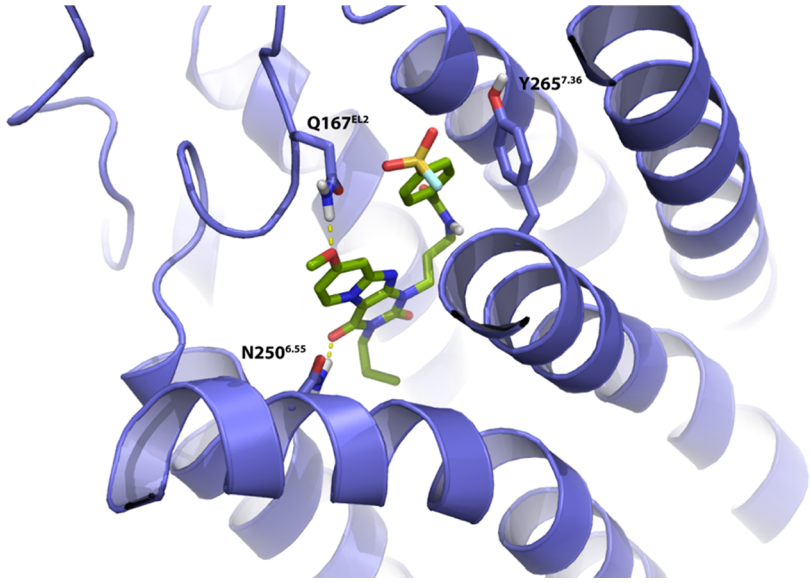

Figure 6. Proposed binding mode of compound **17b** (green carbon sticks) in a homology model (violet ribbons) of the hA_3AR. The hA_3AR homology model was based on the high-resolution antagonist-bound crystal structure of the adenosine A_{2A} receptor (PDB: 4EIY[27]). Atom color code: red = oxygen, blue = nitrogen, white = hydrogen, yellow = sulfur, cyan = fluorine. Hydrogen bonds between the ligand and receptor are indicated by yellow dashed lines. Residue $Y265^{7.36}$ is in the proximity of the fluorosulfonyl warhead.

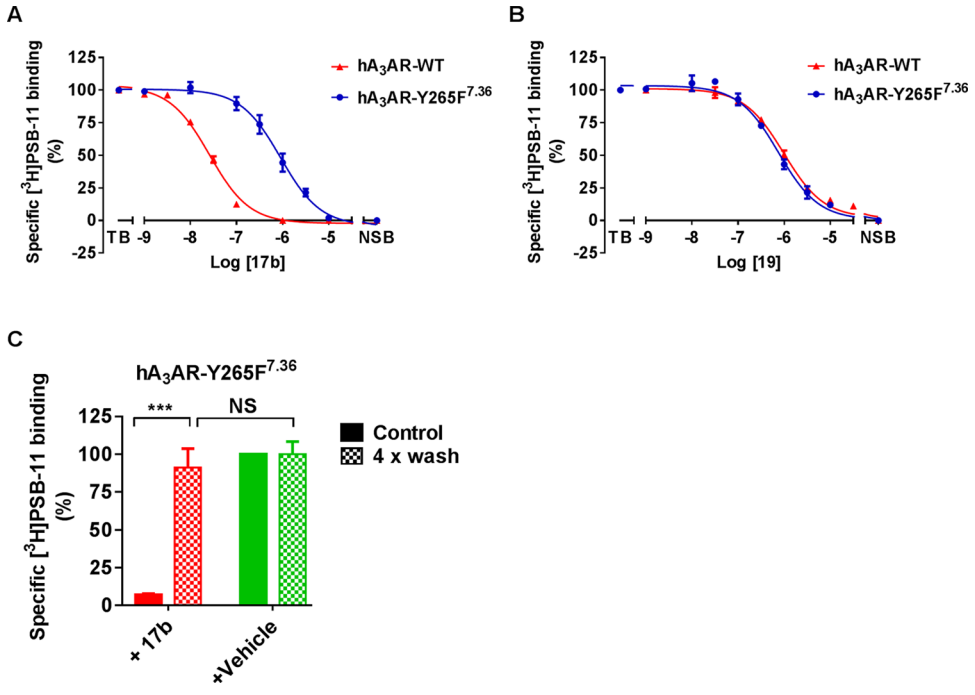

Figure 7. (A, B) Displacement of specific [^{3}H]PSB-11 binding from transiently transfected hA_3AR-WT and hA_3AR-$Y265F^{7.36}$ at 25 °C by compound **17b** (A) and **19** (B) during incubation of 2 h. (C) hA_3AR-$Y265F^{7.36}$ cell membranes were pretreated with buffer (vehicle) or 10 × IC_{50} of compound **17b** for 2 h followed by no washing (control) or four-cycle washing treatment (4× wash) before being exposed to [^{3}H]PSB-11. Data represent the mean ± SEM of three individual experiments performed in duplicate, normalized to the vehicle (set at 100%). NS: no significant difference between groups; ***Significant difference between groups ($P < 0.001$); Student's *t*-test.

antagonism. The Schild plot showed that both antagonists inhibited receptor activation in a competitive manner, with their Schild-slopes close to unity (1.1 ± 0.1 for **17b**, 1.0 ± 0.1 for **19**, Table 3). In addition, **19**'s pA_2 value was in agreement with that from the preincubation experiments (6.2 ± 0.1, Table 3), and the pA_2 value of **17b** was also comparable with its pK_i value (7.4 ± 0.1 vs 8.0 ± 0.05). Taken together, both ligands fully competed with 2-Cl-IB-MECA bound to the hA_3AR. Notably, it is likely that the insurmountable behavior relates to the covalent binding of **17b** due to an irreversible blockade that reduces the total receptor population available.

*Binding Model for **17b** in the hA_3AR Receptor-Binding Pocket.* To examine the interaction between receptor residues possibly involved in covalent binding, we docked **17b** into a ligand optimized homology model on the basis of the A_{2A} receptor crystal structure (PDB: 4EIY[27]), as described

DOI: 10.1021/acs.jmedchem.8b02026
J. Med. Chem. 2019, 62, 3539−3552

previously.[7] As detailed in Figure 6, the core structure of compound **17b** interacted with the TM3, TM6, and EL2 regions. Additionally, the carbonyl-oxygen at the C^4-position participated in H-bond formation with residue $N250^{6.55}$ and the methoxyl moiety at the C^8-position functioned as H-bond acceptor with $Q167^{EL2}$. Interestingly, the latter is a unique residue in the hA_3AR, as it is not conserved in other subtypes of adenosine receptors. Due to the flexibility of the three carbon linkers, the tyrosine residue $Y265^{7.36}$ is in close proximity of the ligand, and could therefore interact with the 4-fluorosulfonylbenzoic warhead to form a covalent sulfonyl amide. Similarly, the same residue $Y271^{7.36}$ located within the human adenosine A_1 receptor has also been reported to covalently interact with the fluorosulfonyl warhead of compound **2**.[11] Comparison of the binding modes of compound **2** and ligand **17b** in an A_1/A_3 receptor overlay showed that key interactions between ligands and binding sites are preserved, such as a hydrogen bond with $N^{6.55}$ (Figure S1).

$Y265^{7.36}$ as an Anchor Point for the Covalent Bond. Based on the docking study, we postulated that $Y265^{7.36}$ is the anchor point for covalent bond formation. To investigate our hypothesis this tyrosine was mutated to phenylalanine (hA_3AR-$Y265F^{7.36}$), to remove the nucleophilic reactivity of the phenolic hydroxyl group. First, we performed standard [^{3}H]PSB-11 displacement assays to investigate the binding affinity of **17b** and **19** using CHO-K1 cell membranes transiently transfected with either wild type (hA_3AR-WT) or mutant receptors (hA_3AR-$Y265F^{7.36}$). As shown in Table 2 and Figure 7, the affinity of control compound **19** on hA_3AR-$Y265F^{7.36}$ (pIC_{50} = 6.09 ± 0.11) was similar to the affinity to hA_3AR-WT (pIC_{50} = 5.95 ± 0.03), indicating that the mutation has no impact on the binding affinity of the reversible ligand. In marked contrast, **17b**'s affinity was decreased nearly 43-fold relative to the WT, from an IC_{50} value of 27 to 1072 nM, indicative of the loss of irreversible interaction. Moreover, there were no marked affinity differences on hA_3AR-$Y265F^{7.36}$ between **17b** and **19**. This suggests that the chemically dissimilar ligands **17b** (reactive) and **19** (nonreactive) exhibit a similar binding interaction with hA_3AR-$Y265F^{7.36}$. We thus speculate that the amino acid in position 7.36 plays a prominent role in the covalent bond formation between the fluorosulfonyl warhead and the receptor. To support this idea, we repeated the washout assay on hA_3AR-$Y265F^{7.36}$. Membranes treated with **17b** at 10-fold IC_{50} inhibited the specific [^{3}H]PSB-11 binding to 7.2 ± 0.6%. After extensive washing, hA_3AR-$Y265F^{7.36}$ showed a complete recovery of [^{3}H]PSB-11 binding to 91 ± 2% (Figure 7C). This full recovery for mutant hA_3AR-$Y265F^{7.36}$ is in sharp contrast to the findings in the wild-type washout assay (Figure 4), indicating that $Y265F^{7.36}$ completely prevented the wash-resistant bond formation. In other words, $Y265^{7.36}$ is the unique amino acid residue involved in the covalent attachment of **17b**'s fluorosulfonyl group within the hA_3AR binding pocket. A similar approach was also adopted to pinpoint the anchor point between covalent probes and other subtypes of GPCRs, such as the adenosine A_{2A} receptor,[21] mGlu2 receptor,[23] and cannabinoid CB_1 receptor.[28]

17b can be a useful structural biology tool as it would be expected to stabilize the 7TM domain in its inactive state, thereby potentially facilitating crystallization of the receptor material. This could be highly valuable for the structure elucidation of the hA_3AR, which up to now remains unreported. Furthermore, understanding the precise molecular interactions between the ligand and the receptor may stimulate the more rational design of novel ligands. Such ligands may have improved receptor subtype selectivity, fewer undesirable side effects, and enhanced potency and efficacy, leading to potentially attractive therapeutic agents that produce their effects by modulating the functionality of the adenosine system. Given that GPCR-targeted covalent drugs went through clinical success across various indications,[29] our covalent compound **17b** may serve as a probe to explore the problematic translation of hA_3AR ligands into the clinical utility in certain disease states such as eye disorder glaucoma, in which an increased A_3 adenosine receptor mRNA and protein levels have been detected.

CONCLUSIONS

By introducing a reactive sulfonyl fluoride warhead onto the 1-benzyl-3-propyl-1*H*,3*H*-pyrido [2,1-*f*]purine-2,4-dione scaffold, we designed and synthesized a series of novel covalent hA_3AR antagonists. Compound **17b** acted as the most potent antagonist, with a time-dependent apparent affinity in the low nanomolar range. Meanwhile, we removed the warhead and inserted a methylsulfonyl moiety into the scaffold, to obtain ligand **19** as a reversible control compound. Ligand **17b** was then validated as a covalent antagonist through its wash-resistant nature and insurmountable antagonism in [^{35}S]GTPγS binding assays. In silico homology-docking suggested that $Y265^{7.36}$ is responsible for the covalent interaction. Site-directed mutagenesis showed that removal of the nucleophilic tyrosine phenolic hydroxyl group resulted in the complete loss of covalent binding, validating that $Y265^{7.36}$ is the only anchor point of reactive covalent ligand **17b**. The results contribute to a better understanding of pharmacological behaviors caused by covalent interaction with GPCRs. In the end, we developed a structured approach to quickly obtain a well-defined covalent ligand. Besides, we envisioned that a methylsulfonyl replacement would be suitable for providing a nonreactive sulfonyl-bearing control compound. The rational design of covalent probes may have further value in receptor structure elucidation or in new technologies such as affinity-based protein profiling[15,30] with the perspective of imaging or structurally probing GPCRs.

EXPERIMENTAL SECTION

Chemistry. All solvents and reagents were purchased from commercial sources and were of analytical grade. Demineralized water is simply referred to as H_2O, and was used in all cases unless stated otherwise (i.e., brine). ^{1}H were recorded on a Bruker AV 400 liquid spectrometer (^{1}H NMR, 400 MHz) at ambient temperature and ^{13}C NMR spectra were recorded on a Bruker AV 600 liquid spectrometer (^{13}C NMR, 125 MHz) at indicated temperature. Chemical shifts are reported in parts per million (ppm), using residual solvent as the internal reference in all cases. The values are given in δ scale. Coupling-constants are reported in Hz and are designated as *J*. Analytical purity of the final compounds was determined by high-performance liquid chromatography (HPLC) with a Phenomenex Gemini 3 μm C18 110 Å column (50 × 4.6 mm, 3 μm), measuring UV absorbance at 254 nm. Sample preparation and the HPLC method were as follows: 0.3−1.0 mg of compound was dissolved in 1 mL of a 1:1:1 mixture of MeCN/H_2O/*t*BuOH and eluted from the column within 15 min at a flow rate of 1.3 mL min^{-1} with a three-component system of H_2O/MeCN/1% trifluoroacetyl (TFA) in H_2O. The elution method was set up as follows: 1−4 min isocratic system of H_2O/MeCN/1% TFA in H_2O, 80:10:10, from the 4th min, a gradient was applied from 80:10:10 to 0:90:10 within 9 min, followed by 1 min of equilibration at 0:90:10 and 1 min at

DOI: 10.1021/acs.jmedchem.8b02026
J. Med. Chem. 2019, 62, 3539−3552

80:10:10. All final compounds showed a single peak at the designated retention time and are at least 95% pure. Liquid chromatography–mass spectrometry (LC–MS) analyses were performed using a Thermo Finnigan Surveyor–LCQ Advantage Max LC–MS system and a Gemini C18 Phenomenex column (50 × 4.6 mm^2, 3 μm). High-resolution mass spectrometry (HRMS) analyses were performed using a Thermo Scientific LTQ Orbitrap XL Hybrid Ion Trap-Orbitrap Mass Spectrometer. The sample preparation was the same as for HPLC and HRMS analyses. The compounds were eluted from the column within 15 min after injection, with a three-component system of H_2O/MeCN/0.2% TFA in H_2O, decreasing polarity of the solvent mixture in time from 80:10:10 to 0:90:10. Thin-layer chromatography (TLC) was routinely performed to monitor the progress of reactions, using aluminum-coated Merck silica gel F254 plates. Purification by column chromatography was achieved using the Grace Davison Davisil silica column material (LC60A 30–200 μm). Solutions were concentrated using a Heidolph Laborota W8 2000 efficient rotary evaporation apparatus. All reactions in the synthetic routes were performed under a nitrogen atmosphere unless stated otherwise. The procedure for a series of similar compounds is given as a general procedure for all within that series, annotated by the numbers of the compounds.

1-Benzyl-8-methoxy-3-propyl-1*H*,3*H*-pyrido[2,1-*f*]purine-2,4-dione (1).[7,8] To a stirred suspension of **6** (6.0 g, 19 mmol, 1.0 equiv) in MeCN (120 mL) were added 1-bromopropane (5.6 mL, 57 mmol, 3.0 equiv) and DBU (50 mL, 57 mmol, 3.0 equiv). This mixture was stirred at 70 °C overnight. The conversion of the starting material was confirmed by TLC (2% MeOH in CH_2Cl_2) and the solvent was removed under vacuum. The residue was suspended in CH_2Cl_2 (200 mL) and the organic phase was washed with 1 M HCl (200 mL), H_2O (200 mL), and brine (200 mL), dried over $MgSO_4$, filtered, and concentrated in vacuo. The crude was purified by column chromatography (0.5% MeOH in CH_2Cl_2) to obtain **1** as a white solid (5.0 g, 14 mmol, 73%). ^{1}H NMR (400 MHz, $CDCl_3$): δ 8.82 (d, J = 7.6 Hz, 1H), 7.58–7.51 (m, 2H), 7.34–7.22 (m, 3H), 6.98 (d, J = 2.0 Hz, 1H), 6.74 (dd, J = 7.4, 2.2 Hz, 1H), 5.36 (s, 2H), 4.04–3.97 (m, 2H), 3.92 (s, 3H), 1.76–1.65 (m, 2H), 0.97 (t, J = 7.4 Hz, 3H)

6-Amino-1-benzyl-1,3-dihydropyrimidine-2,4-dione (5).[7,8] The synthesis of the compounds was performed as adapted from the procedure reported before.[7,8] Benzylurea (**3**) (25 g, 167 mmol, 1.0 equiv) and **4** (16 g, 191 mmol, 1.1 equiv) were dissolved in acetic anhydride (100 mL). This mixture was stirred at 80 °C for 2 h. After the mixture was cooled to room temperature, diethyl ether (150 mL) was added followed by 1 h of stirring at room temperature. The precipitate was filtered off and suspended in a mixture of EtOH (75 mL) and H_2O (150 mL). This mixture was heated to 85 °C and 3 M NaOH (aq.) (50 mL) was added dropwise. After 1 h, the mixture was concentrated and neutralized by the dropwise addition of HCl (37%). The precipitate was filtered off and washed with acetone, obtaining **5** as a white solid (9.0 g, 42 mmol, 25%). ^{1}H NMR (400 MHz, DMSO-d_6): δ 10.42 (brs, 1H), 7.48–7.08 (m, 5H), 6.85 (brs, 2H), 5.03 (s, 2H), 4.60 (s, 1H)

1-Benzyl-8-methoxy-1*H*,3*H*-pyrido[2,1-*f*]purine-2,4-dione (6).[7,8] To the intermediate (**5**) (9.0 g, 42 mmol, 1.0 equiv) and NBS (15 g, 83 mmol, 2.0 equiv) was added MeCN (100 mL). This mixture was stirred at 80 °C. After 1.5 h, the conversion of the starting material was confirmed by TLC (10% MeOH in CH_2Cl_2), 4-methoxypyridine (13 g, 125 mmol, 3.0 equiv) was added and the reaction mixture was stirred at 80 °C for 4.5 h. After cooling to room temperature, the precipitate was filtered off and washed with diethyl ether and MeOH, yielding product **6** as a white solid (8.5 g, 26 mmol, 64%). ^{1}H NMR (400 MHz, DMSO-d_6): δ 11.31 (br s, 1H), 8.70 (d, J = 7.2 Hz, 1H), 7.38–7.16 (m, 6H), 6.90 (dd, J = 7.4, 2.2 Hz, 1H), 5.18 (s, 2H), 3.89 (s, 3H)

8-Methoxy-3-propyl-1*H*,3*H*-pyrido[2,1-*f*]purine-2,4-dione (7).[7,8] To a mixture of intermediate **1** (1.1 g, 3.0 mmol, 1.0 equiv), $Pd(OH)_2$/C (2.0 g, 14 mmol, 1.0 equiv), and ammonium formate (0.20 g, 3.0 mmol, 1.0 equiv) was added EtOH (250 mL). During the reaction, five portions of ammonium formate (0.20 g, 3.0 mmol, 1.0 equiv) was added, after which completion of the reaction was observed by TLC (5% MeOH in CH_2Cl_2). The reaction was filtered over Celite and the residue was extracted with hot DMF. Purification of the crude product was performed by column chromatography using 2–10% MeOH in CH_2Cl_2 to obtain **5** as a white solid (0.30 g, 1.2 mmol, 40%). ^{1}H NMR (400 MHz, DMSO-d_6): δ 12.05 (s, 1H), 8.73 (d, J = 7.2 Hz, 1H), 7.12 (d, J = 2.0 Hz, 1H), 6.89 (dd, J = 7.4, 2.6 Hz, 1H), 3.90 (s, 3H), 3.85–3.78 (m, 2H), 1.64–1.52 (m, 2H), 0.88 (t, J = 7.4 Hz, 3H)

General Procedure for the Synthesis of Fluorosulfonylbenzoic Acids (9a,b). To a solution of chlorosulfonylbenzoic acid (**8a,b**) (2.2 g, 10 mmol, 1.0 equiv) in dioxane (25 mL) was added a solution of HF/KF (15 mL, 2.0 M, 3.0 equiv). The mixture was stirred at room temperature. After 1 h, the reaction mixture was diluted with EtOAc (80 mL). The organic phase was washed with H_2O (50 mL), dried over $MgSO_4$, filtered, and concentrated in vacuo.

*3-(Fluorosulfonyl)benzoic Acid (**9a**).* White solid (1.9 g, 8.7 mmol, 87%). ^{1}H NMR (400 MHz, DMSO-d_6): δ 8.47–8.44 (m, 2H), 8.4 (d, J = 8.0 Hz, 1H), 7.94 (t, J = 7.6 Hz, 1H).

*4-(Fluorosulfonyl)benzoic Acid (**9b**).* White solid (2.0 g, 9.0 mmol, 90%). ^{1}H NMR (400 MHz, DMSO-d_6): δ 13.86 (s, 1H), 8.28 (s, 4H)

General Procedure for the Synthesis of Bromoalkyl (fluorosulfonyl)benzoates (11a–c and 12a–c). A mixture of thionyl chloride (8 mL) and fluorosulfonylbenzoic acid (**9a,b**) (1 equiv) was refluxed at 75 °C for 3 h. The solvent was removed under vacuum and the product was used in the next step without further analysis. Dry dioxane (6 mL) was added to the (fluorosulfonyl)-benzoyl chloride (**10a,b**). To this solution, the corresponding bromoalkylalcohol (0.85 equiv) was added and the mixture was refluxed overnight. After the completion of the reaction was observed by TLC (CH_2Cl_2), the volatiles were removed in vacuo and the crude product was purified by column chromatography using CH_2Cl_2 as an eluent to afford the products.

*2-Bromoethyl-4-(fluorosulfonyl)benzoate (**11a**).* Colorless oil (0.088 g, 0.28 mmol, 23%) ^{1}H NMR (400 MHz, DMSO-d_6): δ 8.31 (d, J = 8.2 Hz, 2H), 8.11 (d, J = 8.5 Hz, 2H), 4.69 (t, J = 5.9 Hz, 2H), 3.67 (t, J = 5.9 Hz, 2H).

*3-Bromopropyl-4-(fluorosulfonyl)benzoate (**11b**).* White solid (2.0 g, 6.2 mmol, 50%) ^{1}H NMR (400 MHz, $CDCl_3$): δ 8.27 (d, J = 8.4 Hz, 2H), 8.09 (d, J = 8.4 Hz, 2H), 4.54 (t, J = 6.0 Hz, 2H), 3.54 (d, J = 6.4 Hz, 2H), 2.35 (m, 2H).

*4-Bromobutyl-4-(fluorosulfonyl)benzoate (**11c**).* White solid (0.30 g, 0.89 mmol, 45%) compound was used without further purification.

*2-Bromoethyl-3-(fluorosulfonyl)benzoate (**12a**).* Colorless oil (0.51 g, 1.7 mmol, 55%) ^{1}H NMR (400 MHz, $CDCl_3$): δ 8.69 (s, 1H), 8.47 (d, J = 7.6 Hz, 1H), 8.25–8.20 (m, 1H), 7.78 (t, J = 8.0 Hz, 1H), 4.71 (t, J = 6.0 Hz, 2H), 3.68 (t, J = 6.0 Hz, 2H).

*3-Bromopropyl-3-(fluorosulfonyl)benzoate (**12b**).* Colorless oil (0.12 g, 0.38 mmol, 23%) ^{1}H NMR (400 MHz, $CDCl_3$) δ 8.65 (t, J = 1.6 Hz, 1H), 8.44 (d, J = 7.8 Hz, 1H), 8.21 (d, J = 8.0 Hz, 1H), 7.76 (t, J = 7.9 Hz, 1H), 4.55 (t, J = 6.1 Hz, 1H), 3.55 (t, J = 6.4 Hz, 1H), 2.37 (p, J = 6.3 Hz, 1H).

*4-Bromobutyl-3-(fluorosulfonyl)benzoate (**12c**).* Colorless Oil (0.84 g, 2.5 mmol, 83%,) ^{1}H NMR (400 MHz, $CDCl_3$): δ 8.65 (s, 1H), 8.45 (d, J = 8.0 Hz, 1H), 8.21 (d, J = 8.0 Hz, 1H), 7.78 (t, J = 7.6 Hz, 1H), 4.44 (t, J = 6.0 Hz, 2H), 3.50 (t, J = 6.4 Hz, 2H), 2.11–1.85 (m, 4H).

General Procedure for the Synthesis of 13a–c and 14a–c. The synthesis of these compounds was adapted from the conditions previously described by Priego et al.[6] The scaffolds 8-methoxy-3-propyl-1*H*,3*H*-pyrido[2,1-*f*]purine-2,4-dione **7** (1.0 equiv) and K_2CO_3 (1.6 equiv) were suspended in anhydrous DMF. The mixture was added dropwise to a stirred solution of the corresponding bromoalkyl (fluorosulfonyl)benzoate (**11a–c** or **12a–c**) (1.0 equiv) in anhydrous DMF (4 mL). The reaction was stirred at 50 °C overnight. After the conversion was observed by TLC, an excess amount of CH_2Cl_2 was added. Then the mixture was washed with 1 M HCl (aq.), water, and brine. The organic layer was dried over $MgSO_4$, filtered, and concentrated in vacuo. The crude product was

DOI: 10.1021/acs.jmedchem.8b02026
J. Med. Chem. 2019, 62, 3539–3552

purified by column chromatography, followed by prep TLC to further purify the compound if necessary.

*2-(8-Methoxy-2,4-dioxo-3-propyl-3,4-dihydropyrido[2,1-f]-purine-1(2H)-yl)ethyl 4-(fluorosulfonyl)benzoate (**13a**).* Prepared from **11a** and purified by column chromatography (1% CH_3OH in CH_2Cl_2) to give the desired product as a white solid (0.038 g, 0.07 mmol, 52%). ^1H NMR (400 MHz, $CDCl_3$): δ 8.80 (d, J = 8.0 Hz, 1H), 8.17 (d, J = 8.0 Hz, 2H), 7.98 (d, J = 8.4 Hz, 2H), 6.76−6.73 (m, 2H), 4.78 (t, J = 4.8 Hz, 2H), 4.64 (t, J = 5.2 Hz, 2H), 4.00 (t, J = 7.6 Hz, 2H), 3.89 (s, 3H), 1.73−1.62 (m, 2H), 0.95 (t, J = 7.2 Hz, 3H). MS: $[ESI + H]^+$: 505.1. HPLC: 9.99 min

*3-(8-Methoxy-2,4-dioxo-3-propyl-3,4-dihydropyrido[2,1-f]-purine-1(2H)-yl)propyl 4-(fluorosulfonyl)benzoate (**13b**).* Prepared from **11b** and purified by column chromatography (1% CH_3OH in CH_2Cl_2) to give the desired product as a white solid (0.096 g, 0.19 mmol, 76%). ^1H NMR (400 MHz, $CDCl_3$): δ 8.76 (d, J = 7.2 Hz, 1H), 8.23 (d, J = 8.0 Hz, 2H), 8.06 (d, J = 8.4 Hz, 2H), 6.77 (d, J = 2.4 Hz, 1H), 6.73 (dd, J = 7.2, 2.4 Hz, 1H), 4.50 (t, J = 6.0 Hz, 2H), 4.41 (t, J = 6.8 Hz, 2H), 4.00 (t, J = 7.2 Hz, 2H), 3.90 (s, 3H), 2.38 (pentet, J = 6.0 Hz, 2H), 1.71 (sextet, J = 7.2 Hz, 2H), 0.99 (t, J = 7.6 Hz, 3H). MS: $[ESI + H]^+$: 519.1. HPLC: 10.18 min

*4-(8-Methoxy-2,4-dioxo-3-propyl-3,4-dihydropyrido[2,1-f]-purine-1(2H)-yl)butyl 4-(fluorosulfonyl)benzoate (**13c**).* Prepared from **11c** and purified by column chromatography (2% CH_3OH in CH_2Cl_2) to give the desired product as a white solid (0.010 g, 0.019 mmol, 5.2%) ^1H NMR (400 MHz, $CDCl_3$): δ 8.83 (dd, J = 7.6, 0.8 Hz, 1H), 8.27 (d, J = 8.0 Hz, 2H), 8.07 (d, J = 8.8 Hz, 2H), 6.93 (d, J = 2.4 Hz, 1H), 6.76 (dd, J = 7.6, 2.4 Hz, 1H), 4.46 (t, J = 6.4 Hz, 2H), 4.28 (t, J = 6.8 Hz, 2H), 4.02 (t, J = 7.2 Hz, 2H), 3.93 (s, 3H), 2.05−1.90 (m, 4H), 1.77−1.68 (m, 2H), 0.99 (t, J = 7.2 Hz, 3H). MS: $[ESI + H]^+$: 533.1. HPLC: 9.40 min

*2-(8-Methoxy-2,4-dioxo-3-propyl-3,4-dihydropyrido[2,1-f]-purine-1(2H)-yl)ethyl 3-(fluorosulfonyl)benzoate (**14a**).* Prepared from **12a** and without purification to give the desired product as a white solid (0.19 g, 0.36 mmol, 57%). ^1H NMR (400 MHz, $CDCl_3$): δ 8.80 (d, J = 7.2 Hz, 1H), 8.51 (s, 1H), 8.36 (d, J = 7.6 Hz, 1H), 8.14−8.09 (m, 1H), 7.66 (t, J = 7.8 Hz, 1H), 6.84 (d, J = 2.4 Hz, 1H), 6.74 (dd, J = 7.6, 2.6 Hz, 1H), 4.78 (t, J = 4.8 Hz, 2H), 4.65 (t, J = 4.8 Hz, 2H), 4.04−3.97 (m, 2H), 3.90 (s, 3H), 1.68 (sextet, J = 7.6 Hz, 2H), 0.96 (t, J = 7.4 Hz, 3H). MS: $[ESI + H]^+$: 505.1. HPLC: 8.47 min

*3-(8-Methoxy-2,4-dioxo-3-propyl-3,4-dihydropyrido[2,1-f]-purine-1(2H)-yl)propyl 3-(fluorosulfonyl)benzoate (**14b**).* Prepared from **12b** and purified by column chromatography (1% CH_3OH in CH_2Cl_2) to give the desired product as a white solid (0.035 g, 0.068 mmol, 34%). ^1H NMR (400 MHz, $CDCl_3$): δ 8.74 (d, J = 7.6 Hz, 1H), 8.65 (s, 1H), 8.36 (d, J = 8.0 Hz, 1H), 8.18 (d, J = 8.0 Hz, 1H), 7.73 (t, J = 8.0 Hz, 1H), 6.86 (d, J = 2.0 Hz, 1H), 6.72 (dd, J = 7.2, 2.4 Hz, 1H), 4.51 (t, J = 6.0 Hz, 2H), 4.41 (t, J = 6.0 Hz, 2H), 3.99 (t, J = 7.6 Hz, 2H), 3.91 (s, 3H), 2.39 (pentet, J = 6.0 Hz, 2H), 1.70 (sextet, J = 7.6 Hz, 2H), 0.98 (t, J = 7.6 Hz, 3H). MS: $[ESI + H]^+$: 519.1. HPLC: 8.84 min

*4-(8-Methoxy-2,4-dioxo-3-propyl-3,4-dihydropyrido[2,1-f]-purine-1(2H)-yl)butyl 3-(fluorosulfonyl)benzoate (**14c**).* Prepared from **12c** and purified by column chromatography (first 30% DCM in EtOAc). Further purification by another column (4:1 = methyl *tert*-butyl ether/petroleum ether) gives the desired product as a white solid (0.20 g, 0.37 mmol, 38%). ^1H NMR (400 MHz, $CDCl_3$): δ 8.85 (d, J = 7.2 Hz, 1H), 8.67 (s, 1H), 8.45 (d, J = 8.0 Hz, 1H), 8.21 (d, J = 8.0 Hz, 1H), 7.75 (t, J = 8.0 Hz, 1H), 6.97 (d, J = 2.4 Hz, 1H), 6.77 (dd, J = 7.2, 2.4 Hz, 1H), 4.49 (t, J = 6.4 Hz, 2H), 4.30 (t, J = 7.2 Hz, 2H), 4.08−4.01 (m, 2H), 3.95 (s, 3H), 2.10−2.00 (m, 2H), 2.00−1.89 (m, 2H), 1.81−1.69 (m, 2H), 1.01 (t, J = 7.2 Hz, 3H). MS: $[ESI + H]^+$: 533.1. HPLC: 9.14 min

General Procedure for the Synthesis of 1-(2-(1,3-Dioxoisoindolin-2-yl)alkyl)-8-methoxy-3-propyl-1*H*,3*H*-pyrido-[2,1-*f*]purine-2,4-dione (15a−c). To a mixture of the core (**7**) (0.8 mmol, 1 equiv), *N*-(bromoalkyl)phthalimide (1.2 mmol, 1.5 equiv), and K_2CO_3 (1.2 mmol, 1.5 equiv) was added anhydrous DMF (8 mL). The mixture was refluxed at 100 °C. After completion of the reaction, monitored by TLC (1% MeOH in CH_2Cl_2), the mixture was concentrated in vacuo and diluted with EtOAc (30 mL). The organic layer was washed with H_2O (3 × 30 mL) and brine (15 mL), and dried over $MgSO_4$. The solvent was evaporated under reduced pressure and the residue was purified by column chromatography using 1% MeOH as an eluent to give **15a−c** as solids.

*1-(2-(1,3-Dioxoisoindolin-2-yl)ethyl)-8-methoxy-3-propyl-1H,3H-pyrido-[2,1-f]purine-2,4-dione (**15a**).* Prepared from *N*-(2-bromoethyl)phthalimide and purified by column chromatography to give the desired product as a white solid (0.20 g, 0.44 mmol, 5%). ^1H NMR ($CDCl_3$): δ 8.77 (d, J = 6.8 Hz, 1H), 7.73 (s, 2H), 7.64 (s, 2H), 6.69 (d, J = 14.0 Hz, 2H), 4.53 (s, 2H), 4.17 (s, 2H), 3.89 (d, J = 6.2 Hz, 2H), 3.85 (s, 3H), 1.58−1.45 (m, 3H), 0.86 (t, J = 7.2 Hz, 3H).

*1-(2-(1,3-Dioxoisoindolin-2-yl)propyl)-8-methoxy-3-propyl-1H,3H-pyrido-[2,1-f]purine-2,4-dione (**15b**).* Prepared from *N*-(3-bromoethyl)phthalimide and purified by column chromatography to give the desired product as a yellow solid (0.31 g, 0.66 mmol, 66%). ^1H NMR (400 MHz, $CDCl_3$): δ 8.81−8.75 (m, 1H), 7.86−7.76 (m, 2H), 7.73−7.61 (m, 2H), 6.80 (s, 1H), 6.72 (dd, J = 7.2, 2.4 Hz, 1H), 4.29 (t, J = 6.8 Hz, 2H), 4.04−3.93 (m, 2H), 3.90 (s, 3H), 3.86−3.78 (m, 2H), 2.35−2.20 (m, 2H), 1.78−1.60 (m, 2H), 1.06−0.87 (m, 3H).

*1-(2-(1,3-Dioxoisoindolin-2-yl)butyl)-8-methoxy-3-propyl-1H,3H-pyrido-[2,1-f]purine-2,4-dione (**15c**).* Prepared from *N*-(4-bromoethyl)phthalimide and purified by column chromatography to give the desired product as a white solid (0.37 g, 0.76 mmol, 96%). ^1H NMR (400 MHz, $CDCl_3$): δ 8.82 (d, J = 7.2 Hz, 1H), 7.82 (dd, J = 5.2, 2.8 Hz, 2H), 7.70 (dd, J = 5.2, 2.8 Hz, 2H), 6.93 (d, J = 2.4 Hz, 1H), 6.74 (dd, J = 7.2, 2.4 Hz, 1H), 4.22 (d, J = 7.2 Hz, 2H), 4.04−3.96 (m, 2H), 3.92 (s, 3H), 3.75 (d, J = 7.2 Hz, 2H), 1.95−1.85 (m, 2H), 1.85−1.77 (m, 2H), 1.74−1.65 (m, 3H), 0.97 (d, J = 7.6 Hz, 3H).

General Procedure for the Synthesis of 1-(2-Aminoalkyl)-8-methoxy-3-propyl-1*H*,3*H*-pyrido-[2,1-*f*]purine-2,4-dione (16a−c). To a stirred suspension of **15a−c** (0.66 mmol, 1 equiv) in MeOH (8 mL) was added excess hydrazine monohydrate (4.8 mL, 99 mmol). The mixture was stirred for 2−4 h at reflux. After conversion of the starting material, the mixture was cooled to room temperature. The solvents were removed under vacuum and the residue was dissolved in 2 M NaOH (aq.) (25 mL). This aqueous phase was extracted three times with CH_2Cl_2 (25 mL). The organic layers were combined, dried over $MgSO_4$, and concentrated in vacuo to obtain **16a−c**.

*1-(2-Aminoethyl)-8-methoxy-3-propyl-1H,3H-pyrido-[2,1-f]-purine-2,4-dione (**16a**).* Prepared from **15a** and purified by column chromatography to give the desired product as a white solid (0.13 g, 0.39 mmol, 90%). ^1H NMR (400 MHz, $CDCl_3$): δ 8.84 (d, J = 7.6 Hz, 1H), 6.95 (d, J = 2.4 Hz, 1H), 6.75 (dd, J = 7.2, 2.4 Hz, 1H), 4.27 (t, J = 6.4 Hz, 2H), 4.05−3.99 (m, 2H), 3.93 (s, 3H), 3.15 (t, J = 6.4 Hz, 2H), 1.78−1.67 (m, 2H), 0.99 (d, J = 7.6 Hz, 3H).

*1-(3-Aminopropyl)-8-methoxy-3-propyl-1H,3H-pyrido-[2,1-f]-purine-2,4-dione (**16b**).* Prepared from **15b** and purified by column chromatography to give the desired product as a white solid (0.25 g, 0.75 mmol, 97%). ^1H NMR (400 MHz, $CDCl_3$): δ 8.82 (d, J = 7.2 Hz, 1H), 6.95 (d, J = 2.4 Hz, 1H), 6.75 (dd, J = 7.6, 2.4 Hz, 1H), 4.29 (t, J = 6.8 Hz, 2H), 4.07−3.98 (m, 2H), 3.93 (s, 3H), 2.75 (t, J = 6.6 Hz, 2H), 1.98 (p, J = 6.6 Hz, 2H), 1.78−1.65 (m, 2H), 0.99 (t, J = 7.4 Hz, 3H).

*1-(4-Aminobutyl)-8-methoxy-3-propyl-1H,3H-pyrido-[2,1-f]-purine-2,4-dione (**16c**).* Prepared from **15c** and purified by column chromatography to give the desired product as a white solid (0.23 g, 0.66 mmol, 86%). ^1H NMR (400 MHz, $CDCl_3$): δ 8.84 (d, J = 7.6 Hz, 1H), 6.97 (d, J = 2.4 Hz, 1H), 6.75 (dd, J = 7.2, 2.4 Hz, 1H), 4.20 (t, J = 7.2 Hz, 2H), 4.06−3.98 (m, 2H), 3.92 (s, 3H), 2.77 (d, J = 6.8 Hz, 2H), 1.92−1.82 (m, 2H), 1.78−1.66 (m, 2H), 1.63−1.53 (m, 2H), 0.99 (t, J = 7.2 Hz, 3H).

*4-((2-(8-Methoxy-2,4-dioxo-3-propyl-3,4-dihydropyrido[2,1-f]-purin-1(2H)-yl)ethyl)carbamoyl)benzenesulfonyl Fluoride (**17a**).* EDC (0.12 g, 0.60 mmol, 1.2 equiv) was dissolved in $CHCl_3$ (4 mL). To this stirring solution was added the acid (**9a**) (0.11 g, 0.55 mmol, 1.1 equiv). The amine (**16a**) (0.16 g, 0.50 mmol, 1.0 equiv) was suspended in $CHCl_3$ (6 mL) and then was added dropwise via an

DOI: 10.1021/acs.jmedchem.8b02026
J. Med. Chem. 2019, 62, 3539−3552

automatic syringe at a rate of 0.2 mL min^{-1}. The reaction was stirred for 1.5 h at room temperature and monitored by TLC (CH_2Cl_2/acetone = 3:2). After completion, the solvent was removed under vacuum and the residue was redissolved in $CHCl_3$ (40 mL). The organic layer was washed with 1 M HCl (40 mL) and H_2O (2 × 40 mL), dried over $MgSO_4$, and concentrated in vacuo to obtain **17a** as a white solid (0.20 g, 0.39 mmol, 78%). ^1H NMR (400 MHz, $CDCl_3$): δ 8.83 (d, J = 7.2 Hz, 1H), 8.07−8.00 (m, 5H), 6.91 (d, J = 2.4 Hz, 1H), 6.80 (dd, J = 7.2, 2.0 Hz, 1H), 4.62−4.55 (m, 2H), 4.03 (t, J = 7.6 Hz, 2H), 3.95 (s, 3H), 3.94−3.89 (m, 2H), 1.68 (sextet, J = 7.6 Hz, 2H), 0.97 (t, J = 7.2 Hz, 3H). MS: $[ESI + H]^+$: 504.1. HPLC: 7.93 min.

*4-((3(8-Methoxy-2,4-dioxo-3-propyl-3,4-dihydropyrido[2,1-f]-purin-1(2H)yl)propyl)carbamoyl)benzenesulfonyl Fluoride (**17b**).* A suspension of EDC (0.22 g, 0.80 mmol, 1.5 equiv) and **9a** (0.16 g, 0.80 mmol 1.05 equiv) was dissolved in CH_2Cl_2 (4 mL). To this stirring solution amine was added (**16b**) (0.25 g, 0.76 mmol, 1.0 equiv) at room temperature. The reaction was stirred for 2 h and monitored by TLC (3% MeOH in CH_2Cl_2). After completion, the solvent was removed in vacuo and the residue was dissolved in $CHCl_3$ (40 mL). The organic layer was washed with 1 M HCl (40 mL) and twice with H_2O (2 × 40 mL), dried over $MgSO_4$, and concentrated in vacuo. The product was purified by column chromatography using 2% MeOH in CH_2Cl_2 to afford the title compound as a white solid (0.26 g, 0.50 mmol, 66%). ^1H NMR (400 MHz, $CDCl_3$) δ: 8.86 (d, J = 7.2 Hz, 1H), 8.38 (t, J = 5.6 Hz, 1H), 8.25 (d, J = 8.4 Hz, 2H), 8.16 (d, J = 8.4 Hz, 2H), 6.85 (d, J = 2.4 Hz, 1H), 6.81 (dd, J = 7.2, 2.4 Hz, 1H), 4.35 (t, J = 6.0 Hz, 2H), 4.05 (t, J = 7.6 Hz, 2H), 3.92 (s, 3H), 3.47 (q, J = 6.4 Hz, 2H), 2.19−2.13 (m, 2H), 1.73 (sextet, J = 7.6 Hz, 2H), 1.00 (t, J = 7.6 Hz, 3H). ^{13}C NMR (600 MHz, DMSO-d_6, 348 K) δ 164.0, 160.9, 153.4, 150.6, 150.5, 149.1, 141.3, 133.3 (d, J = 96 Hz), 128.5, 127.9, 127.3, 107.0, 99.8, 95.4, 55.7, 41.5, 40.6, 36.8, 27.1, 20.5, 10.6. MS: $[ESI + H]^+$: 518.1. HRMS-ESI^+: $[M + H]^+$ calcd: 518.1510 found: 518.1540, $C_{23}H_{25}O_6N_5FS$. HPLC: 8.27 min.

*4-((4-(8-Methoxy-2,4-dioxo-3-propyl-3,4-dihydropyrido[2,1-f]-purin-1(2H)-yl)butyl)carbamoyl)benzenesulfonyl Fluoride (**17c**).* Acid **9a** (0.11 g, 0.53 mmol, 1.5 equiv) was dissolved in an excess of thionyl chloride (20 mL) at 75 °C under nitrogen for 3 h. After removal of solvent and other volatiles under vacuum, **10a** was obtained as a colorless oil. Subsequently, amine **16c** (0.12 g, 0.35 mmol, 1.0 equiv), K_2CO_3 (0.073 g, 0.53 mmol, 1.5 equiv), and dry DMF were added and the reaction as stirred at 40 °C overnight. After completion of the reaction, 1 M HCl (200 mL) was added and extracted with CH_2Cl_2 (150 mL). The organic layer was washed with water (100 mL) and brine (100 mL). The organic layer was dried, filtered, and concentrated in vacuo. The residue was purified by column chromatography using CH_2Cl_2 with 1% methanol as the eluent to give **17c** as a white solid (5.0 mg, 0.0094 mmol, 4%). ^1H NMR (400 MHz, $CDCl_3$): δ 8.87 (d, J = 7.6 Hz, 1H), 8.17 (d, J = 8.4 Hz, 2H), 8.09 (d, J = 8.4 Hz, 2H), 7.54 (brs, 1H), 6.85 (s, 1H), 6.80 (dd, J = 7.2, 2.4 Hz, 1H), 4.29 (t, J = 7.6 Hz, 2H), 4.06 (t, J = 7.6 Hz, 2H), 3.92 (s, 3H), 3.68 (q, J = 6.0 Hz, 2H), 2.01 (pent, J = 6.8 Hz, 2H), 1.84−1.70 (m, 4H), 1.02 (t, J = 7.6 Hz, 3H). MS: $[ESI + H]^+$: 532.3. HPLC: 8.28 min.

*3-((2-(8-Methoxy-2,4-dioxo-3-propyl-3,4-dihydropyrido[2,1-f]-purin-1(2H)-yl)ethyl)carbamoyl)benzenesulfonyl Fluoride (**18a**).* EDC (0.12 g, 0.60 mmol, 1.2 equiv) was dissolved in $CHCl_3$ (4 mL). To this stirring solution was added acid **9b** (0.11 g, 0.55 mmol, 1.1 equiv). Amine **16a** (0.16 g, 0.50 mmol, 1.0 equiv) was suspended in $CHCl_3$ (6 mL) and then was added dropwise via an automatic syringe at a rate of 0.2 mL min^{-1}. The reaction was stirred for 3 h at room temperature and monitored by TLC (CH_2Cl_2/acetone = 3:2). After completion, the solvent was removed in vacuo and the residue was resolubilized in $CHCl_3$ (40 mL). The organic layer was washed with 1 M HCl (40 mL) and twice with H_2O (2 × 40 mL), dried over $MgSO_4$, and concentrated in vacuo to give **18a** as a white solid (0.17 g, 0.35 mmol, 70%). ^1H NMR (400 MHz, $CDCl_3$): δ 8.81 (d, J = 7.6 Hz, 1H), 8.37 (s, 1H), 8.29 (d, J = 8.0 Hz, 1H), 8.11 (d, J = 7.6 Hz, 1H), 8.04 (br s, 1H), 7.71 (t, J = 8.0 Hz, 1H), 7.02 (d, J = 2.4 Hz, 1H), 6.77 (dd, J = 7.6, 2.4 Hz, 1H), 4.61−4.54 (m, 2H), 4.03 (t, J = 7.6 Hz, 2H), 3.96 (s, 3H), 3.94−3.89 (m, 2H), 1.76−1.63 (m, 2H), 0.97 (t, J = 7.6 Hz, 3H). MS: $[ESI + H]^+$: 504.1. HPLC: 7.67 min.

*3-((3-(8-Methoxy-2,4-dioxo-3-propyl-3,4-dihydropyrido[2,1-f]-purin-1(2H)-yl)propyl)carbamoyl) benzenesulfonyl Fluoride (**18b**).* Acid **9b** (0.42 g, 2.0 mmol, 3.0 equiv) was dissolved in thionyl chloride (20 mL) and stirred for 3 h at 75 °C. The thionyl chloride was evaporated and the residue was co-evaporated twice with toluene. Then, amine **14b** (0.23 mg, 0.7 mmol, 1.00 equiv), K_2CO_3 (0.073 g, 0.53 mmol, 1.5 equiv), and dry DMF were added and the reaction was stirred at 40 °C overnight. 1 M HCl (200 mL) was added and extracted with CH_2Cl_2 (150 mL). The organic layer was washed with water (100 mL) and brine (100 mL). The organic layer was dried, filtered, and concentrated in vacuo. The residue was purified by column chromatography using CH_2Cl_2 with 1% methanol as the eluent to give **18b** as a white solid (0.0050 g, 0.01 mmol, 2.7%). ^1H NMR (400 MHz, $CDCl_3$) δ: 8.88 (d, J = 7.2 Hz, 1H), 8.68 (s, 1H), 8.55−8.50 (m, 2H), 8.20 (d, J = 8.0 Hz, 1H), 7.82 (t, J = 8 Hz, 2H), 7.00 (d, J = 2.4 Hz, 1H), 6.80 (dd, J = 7.2, 2.4 Hz, 1H), 4.33 (t, J = 6.0 Hz, 2H), 4.05 (t, J = 7.6 Hz, 2H), 3.94 (s, 3H), 3.47 (q, J = 6.0 Hz, 2H), 2.17−2.12 (m, 2H), 1.74 (sextet, J = 7.6 Hz, 2H), 1.00 (t, J = 7.6 Hz, 3H). MS: ESI $[M + H]^+$: 518.1 HPLC: 8.28 min.

*3-((4-(8-Methoxy-2,4-dioxo-3-propyl-3,4-dihydropyrido[2,1-f]-purin-1(2H)-yl)butyl)carbamoyl)benzenesulfonyl Fluoride (**18c**).* EDC (0.13 g, 0.69 mmol, 1.2 equiv) was dissolved in CH_2Cl_2 (3 mL). Acid **9b** (0.13 g, 0.63 mmol, 1.1 equiv) was added to this solution and the mixture was stirred. Amine **16c** (0.20 g, 0.57 mmol, 1 equiv) was dissolved in $CHCl_3$ (8 mL) and added dropwise via an automatic syringe at a rate of 0.2 mL min^{-1} to the stirring solution. After 3 h at room temperature, the reaction was completed and the mixture was concentrated in vacuo. The residue was dissolved in CH_2Cl_2 (40 mL) and washed with 1 M HCl (40 mL) and twice with H_2O (2 × 40 mL). The organic layer was dried over $MgSO_4$ and concentrated in vacuo. Purification by column chromatography (CH_2Cl_2/acetone = 3:2) gave **18c** as a white solid (0.14 g, 0.26 mmol, 47%). ^1H NMR (400 MHz, $CDCl_3$): δ 8.84 (d, J = 7.2 Hz, 1H), 8.54 (s, 1H), 8.36 (d, J = 7.6 Hz, 1H), 8.12 (d, J = 7.6 Hz, 1H), 7.72 (t, J = 7.6 Hz, 1H), 7.62 (br s, 1H), 6.84 (s, 1H), 6.80−6.70 (m, 1H), 4.27 (t, J = 7.2 Hz, 2H), 4.04 (t, J = 8.0 Hz, 2H), 3.89 (s, 3H), 3.74−3.60 (m, 2H), 2.07−1.92 (m, 2H), 1.85−1.64 (m, 4H), 0.98 (t, J = 7.2 Hz, 3H). MS: $[ESI + H]^+$: 532.3. HPLC: 8.21 min.

*N-(3-(8-Methoxy-2,4-dioxo-3-propyl-3,4-dihydropyrido[2,1-f]-purin-1(2H)-yl)propyl)-4-(methylsulfonyl)benzamide (**19**).* To a solution of EDC (0.061 g, 0.32 mmol, 1.2 equiv) in $CHCl_3$ (5 mL) was added 4-(methylsulfonyl)benzoic acid (0.060 g, 0.30 mmol, 1.1 equiv). Amine **16b** (0.090 g, 0.27 mmol, 1 equiv) was taken up in $CHCl_3$ (5 mL) and was subsequently added dropwise via an automatic syringe at a rate of 0.15 mL min^{-1}. The reaction was stirred at room temperature and monitored by TLC (4% MeOH in CH_2Cl_2). After 3 h, the reaction was completed and $CHCl_3$ (50 mL) was added. The organic layer was washed with 1 M HCl (60 mL), H_2O (60 mL), and brine (60 mL), dried over $MgSO_4$, and concentrated under vacuum. The product was purified by column chromatography using 2% MeOH in CH_2Cl_2 to afford the title compound (0.075 g, 0.14 mmol, 54%). ^1H NMR (400 MHz, $CDCl_3$): δ 8.86 (d, J = 7.2 Hz, 1H), 8.36 (t, J = 5.6 Hz, 1H), 8.19 (d, J = 8.4 Hz, 2H), 8.09 (d, J = 8.4 Hz, 2H), 6.90−6.71 (m, 2H), 4.45−4.28 (m, 2H), 4.13−3.99 (m, 2H), 3.91 (s, 3H), 3.55−3.41 (m, 2H), 3.11 (s, 3H), 2.27−2.09 (m, 2H), 1.83−1.61 (m, 2H), 1.00 (t, J = 7.4 Hz, 3H). ^{13}C NMR (600 MHz, DMSO-d_6, 318 K): δ 164.7, 161.1, 153.5, 150.7, 150.6, 149.3, 142.8, 138.9, 127.9, 127.5, 126.7, 107.4, 99.9, 95.4, 56.0, 43.2, 41.6, 40.8, 36.8, 27.4, 20.7, 10.9. MS: $[ESI + H]^+$: 514.2. HRMS-ESI^+: $[M + H]^+$ calcd: 518.1760 found: 518.1791, $C_{24}H_{28}O_6N_5S$. HPLC: 6.89 min.

Computational Studies. All calculations were performed using the Schrodinger Suite.[31] Since compound **17b** shares high similarity with the ligands on which we previously published,[7] the same homology model based on the high-resolution antagonist-bound crystal structure of the adenosine A_{2A} receptor (PDB: 4EIY[27]) was used for the docking studies performed here. Based on these proposed

DOI: 10.1021/acs.jmedchem.8b02026
J. Med. Chem. 2019, 62, 3539−3552

docking poses, we used induced fit docking[32] with core constraints on the pyridopurinedione to dock the different ligands.

Biology. [^{3}H]8-Ethyl-4-methyl-2-phenyl-(8*R*)-4,5,7,8-tetrahydro-1*H*-imidazo[2,1-*i*]-purin-5-one ([^{3}H]PSB-11, specific activity 56 Ci mmol^{-1}) was a gift from Prof. C. E. Müller (University of Bonn, Germany). Unlabeled PSB-11, 1-deoxy-1-[6-[3- and 2-chloro-N6-(3-iodobenzyl)-adenosine-5′-*N*-methyluronamide]] (2-Cl-IB-MECA) were purchased from Tocris Ltd. (Abingdon, U.K.). 5′-*N*-Ethylcarboxamidoadenosine (NECA) was purchased from Sigma-Aldrich (Steinheim, Germany). Adenosine deaminase was purchased from Boehringer Mannheim (Mannheim, Germany). Bicinchoninic acid (BCA) and BCA protein assay reagents were purchased from Pierce Chemical Company (Rockford, IL). Chinese hamster ovary (CHO) cells stably expressing the human A_3 adenosine receptor ($CHOhA_3$) were a gift from Dr. K.-N. Klotz (University of Würzburg, Germany). All other chemicals were obtained from standard commercial sources and were of analytical grade.

Cell Culture and Membrane Preparation. Chinese hamster ovary (CHO) cells, stably expressing the human A_3 adenosine receptor ($CHOhA_3$), were cultured and membranes were prepared and stored as previously reported.[7,33] Protein determination was performed based on the bicinchoninic acid (BCA) method.[34]

Y265F$^{7.36}$ Site-Directed Mutagenesis. The single tyrosine mutation introduced in TM7 of the hA_3AR was performed with the QuickChange II Site-Directed Mutagenesis system (Stratagene, Huizen, The Netherlands). The wild-type pcDNA3.1(+)-A_3AR plasmid DNA with N-terminal 3 × HA-tag was used as a template for polymerase chain reaction (PCR) mutagenesis. Mutant primers for directional PCR product cloning were designed using the online Quickchange primer design program (Agilent Technologies, Santa Clara, CA) and obtained from Eurogentec (Maastricht, The Netherlands). Forward primer used for this procedure was 5′-cacagcttgtgctgttcatgggcatcctgct-3′ and the reverse primer was 5′-agcaggatgcccatgaacagcacaagctgtg-3′. All DNA sequences were verified by Sanger sequencing at LGTC (Leiden, The Netherlands).

Transient Expression of Wild Type (WT) and Mutant Receptors in CHO-K1 Cells. CHO-K1 cells were seeded into 150 mm culture dishes to achieve 60% confluence in the presence of 20 mL culture medium consisting of Dulbecco's modified Eagle's medium/F12 (1:1) supplemented with 10% (v/v) newborn calf serum, streptomycin (50 μg mL^{-1}), and penicillin (50 IU mL^{-1}). The cells were transfected approximately 24 h later with plasmid DNA (20 μg of DNA/dish) by the PEI method[35] (PEI/DNA = 3:1) and left for 24 h. Subsequently, the medium was removed and fresh medium containing 5 mM sodium butyrate was added (to enhance the receptor expression level[36]), and cells were grown for an additional 24 h at 37 °C and 5% CO_2. Membrane preparation followed the procedure described above for the CHO cell membranes stably expressing the hA_3AR.[7,33]

Radioligand Displacement Assay. Radioligand displacement experiments were performed as in previously published methods.[7] Membrane aliquots containing 15 μg of protein were incubated in a total volume of 100 μL assay buffer (50 mM Tris−HCl, 5 mM $MgCl_2$, supplemented with 0.01% 3-[(3-cholamidopropyl)-dimethylammonio]-1-propanesulfonate and 1 mM ethylenediaminetetraacetic acid (EDTA), pH 7.4) at 25 °C for 120 min. Displacement experiments were performed using six concentrations of competing antagonist in the presence of ∼10 nM [^{3}H]PSB-11. Nonspecific binding was determined in the presence of 100 μm NECA and represented less than 10% of total binding. Incubation was terminated by rapid filtration performed on 96-well GF/B filter plates (PerkinElmer, Groningen, the Netherlands) in a PerkinElmer Filtermate-harvester (PerkinElmer, Groningen, the Netherlands). After the filter plate was dried at 55 °C for 30 min, the filter-bound radioactivity was determined by scintillation spectrometry using a 2450 MicroBeta^2 Plate Counter (PerkinElmer, Boston, MA).

Radioligand Competition Association Assay. The competition association assay was performed by incubation of ∼10 nM [^{3}H]PSB-11 in the absence or presence of the competing hA_3AR antagonist at its IC_{50} concentration with membrane aliquots. The amount of receptor-bound radioligand was determined at different time points up to 240 min. Incubations were terminated and samples were obtained as described under the Radioligand Displacement Assay.

[^{35}S] GTPγS Binding Assay. The assays were started by adding 15 μg of homogenized CHOhA3 membranes in an ice-cold assay buffer to a total volume of 80 μL containing 50 mM Tris−HCl buffer, 5 mM $MgCl_2$, 1 mM EDTA, 0.05% bovine serum albumin and 1 mM dithiothreitol, 100 mM NaCl, pH 7.4, supplemented with 1 μm GDP and 5 μg saponin. The assays were performed in a 96-well plate format, where stock solutions of the compounds were added to a total volume of 100 μL using an HP D300 Digital Dispenser (Tecan, Männedorf, Switzerland). The final concentration of dimethyl sulfoxide (DMSO) per assay point was ≤0.1%. The basal level of [^{35}S] GTPγS binding was determined in the absence of the ligand, whereas the maximal level of [^{35}S] GTPγS binding was determined in the presence of 10 μm 2-Cl-IB-MECA. For the insurmountability experiments, membrane preparations were preincubated with or without antagonists (0.1-,1-, 3-, 10-fold K_i values) for 60 min at 25 °C, prior to the addition of 2-Cl-IB-MECA (10 μm to 0.1 nM) and 20 μL [^{35}S] GTPγS (final concentration ∼0.3 nM), after which incubation continued for another 30 min at 25 °C. For the surmountability (control) experiments, antagonists (1-, 3-, 10-fold K_i values) and 2-Cl-IB-MECA (10 μm to 0.1 nM) were co-incubated with [^{35}S] GTPγS for 30 min at 25 °C. For all experiments, incubations were terminated and samples were obtained as described under the Radioligand Displacement Assay, using GF/B filters (Whatman International, Maidstone, U.K.).

Data Analysis. All experimental data were analyzed using the nonlinear regression curve fitting program GraphPad Prism 7.0 (GraphPad Software, Inc., San Diego, CA). Data from the radioligand displacement assays were fit into one-site binding mode, and the obtained IC_{50} values were converted into K_i values using the Cheng−Prusoff equation to determine the affinity of the ligands.[37] The observed association rate constants (k_{obs}) derived from both assays were obtained by fitting association data using one-phase exponential association. The dissociation rate constants were obtained by fitting dissociation data to a one phase exponential decay model. The k_{obs} values were converted into association rate constants (k_{on}) using the equation $k_{on} = (k_{obs} - k_{off})/[L]$, where [L] is the amount of radioligand used for the association experiments. Association and dissociation rate constants for unlabeled compounds were calculated by fitting the data into the competition association model using "kinetics of competitive binding".[22]

$$K_A = k_1[L] \times 10^{-9} + k_2$$

$$K_B = k_3[I] \times 10^{-9} + k_4$$

$$S = \sqrt{(K_A - K_B)^2 + 4 \times k_1 \times k_3 \times L \times I \times 10^{-18}}$$

$$K_F = 0.5(K_A + K_B + S)$$

$$K_S = 0.5(K_A + K_B - S)$$

$$Q = \frac{B_{max} \times k_1 \times L \times 10^{-9}}{K_F - K_S}$$

$$Y = Q \times \left(\frac{k_4 \times (K_F - K_S)}{K_F \times K_S} + \frac{k_4 - K_F}{K_F} e^{(-K_F \times X)} - \frac{k_4 - K_S}{K_S} e^{(-K_S \times X)} \right)$$

where X is the time (min), Y is the specific [^{3}H]PSB-11 binding (DPM), k_1 and k_2 are the k_{on} (M^{-1} min^{-1}) and k_{off} (min^{-1}) of [^{3}H]PSB-11, respectively, B_{max} is the total binding (DPM), L is the radioligand concentration (nM), and I is the concentration of the unlabeled competitor (nM). Association and dissociation rate constants for [^{3}H]PSB-11 (k_1 = 0.281 ± 0.04 × 10^8 M^{-1} min^{-1} and k_2 = 0.3992 ± 0.02 min^{-1}) were obtained from Xia et al.[7] With

DOI: 10.1021/acs.jmedchem.8b02026
J. Med. Chem. 2019, 62, 3539−3552

that, the k_3, k_4, and B_{max} were calculated, where k_3 represents the k_{on} (M^{-1} min^{-1}) of the unlabeled ligand, k_4 stands for the k_{off} (min^{-1}) of the unlabeled ligand and B_{max} equals the total binding (DPM). All competition association data were globally fitted. The residence time (RT, in min) was calculated using the equation RT = $1/k_{off}$, as k_{off} values are expressed in min^{-1}. [^{35}S] GTPγS binding curves were analyzed by nonlinear regression using "log (agonist) vs response—variable slope" to obtain potency, inhibitory potency, or efficacy values of agonists and antagonists (EC_{50} and E_{max}, respectively). In the (in)surmountability assays, Schild EC_{50} shift equations were used to obtain Schild-slopes and pA_2 values. All experimental values obtained are means of three independent experiments performed in duplicate.

■ ASSOCIATED CONTENT

Supporting Information

The Supporting Information is available free of charge on the ACS Publications website at DOI: 10.1021/acs.jmedchem.8b02026.

Overlay of a crystal structure of compound **2** bound to human adenosine A_1 receptor (PDB: 5UEN) and a hA_3AR homology model with **17b** docked (PDF)

Homology model of hA_3AR with **17b** (PDB)

Molecular formula strings with bioactivity (CSV)

■ AUTHOR INFORMATION

Corresponding Author

*E-mail: ijzerman@lacdr.leidenuniv.nl. Tel: +31-71-527-4651.

ORCID

Daan van der Es: 0000-0003-3662-8177

Adriaan P. IJzerman: 0000-0002-1182-2259

Author Contributions

X.Y., L.H.H., and A.P.I. conceived the study. L.H.H., D.v.d.E., and A.P.I. supervised the project. Chemical synthesis was designed and supervised by X.Y. and J.P.D.v.V. and performed by J.O., B.J.K., and J.P.D.v.V. The bioassays were supervised by L.H.H and performed by X.Y. The computational work was performed by E.B.L. The manuscript was written by X.Y., L.H.H., D.v.d.E., and A.P.I.

Notes

The authors declare no competing financial interest.

The homology model was based on the crystal structure of the adenosine A_{2A} receptor (PDB: 4EIY). Authors will release the atomic coordinates upon article publication.

■ ACKNOWLEDGMENTS

We thank Prof C. E. Müller (Bonn University, Germany) for her kind help in obtaining [^{3}H]PSB-11, the radiolabeled probe used in this study. We are also thankful to our colleague, Lindsey Burggraaff, for her assistance with computational modeling studies and Ing. G.K. Spijksma for assistance with HRMS. X.Y. is supported by a grant from the Chinese Scholarship Council.

■ ABBREVIATIONS

BCA, bicinchoninic acid; CHO, Chinese hamster ovary; CHO-K1, a subclone from the parental CHO cell line; 2-Cl-IB-MECA, 1-[2-chloro-6-[[(3-iodophenyl)methyl]amino]-9*H*-purin-9-yl]-1-deoxy-*N*-methyl-β-D-ribofuranuronamide; DBU, 1,8-diazabicyclo[5.4.0]undec-7-ene; EDC, 1-ethyl-3-(3-dimethylaminopropyl)carbodiimide; E_{max}, maximum response elicited by an unlabeled ligand in a functional assay (relatively to 2-Cl-IB-MECA) at membranes of CHO cells stably expressing the A_3 adenosine receptor; EtOAc, ethyl acetate; G418, geneticin; GTPγS, guanosine 5′-*O*-[γ-thio]triphosphate; hA_1AR, human A_1 adenosine receptor; hA_3AR, human A_3 adenosine receptor; MeCN, acetonitrile; NECA, 5′-(*N*-ethylcarboxamide)adenosine; PSB-11, 8-Ethyl-4-methyl-2-phenyl-(8*R*)-4,5,7,8-tetrahydro-1*H*- imidazo[2,1-*i*]-purin-5-one

■ REFERENCES

(1) Fredholm, B. B.; IJzerman, A. P.; Jacobson, K. A.; Klotz, K. N.; Linden, J. International Union of Pharmacology. XXV. Nomenclature and classification of adenosine receptors. *Pharmacol. Rev.* **2001**, *53*, 527−552.

(2) Ali, H.; Cunhamelo, J. R.; Saul, W. F.; Beaven, M. A. Activation of phospholipase-C via adenosine receptors provides synergistic signals for secretion in antigen-stimulated Rbl-2h3 cells - evidence for a novel adenosine receptor. *J. Biol. Chem.* **1990**, *265*, 745−753.

(3) Borea, P. A.; Varani, K.; Vincenzi, F.; Baraldi, P. G.; Tabrizi, M. A.; Merighi, S.; Gessi, S. The A_3 adenosine receptor: history and perspectives. *Pharmacol. Rev.* **2015**, *67*, 74−102.

(4) Yang, H.; Avila, M. Y.; Peterson-Yantorno, K.; Coca-Prados, M.; Stone, R. A.; Jacobson, K. A.; Civan, M. M. The cross-species A_3 adenosine-receptor antagonist MRS 1292 inhibits adenosine-triggered human nonpigmented ciliary epithelial cell fluid release and reduces mouse intraocular pressure. *Curr. Eye Res.* **2005**, *30*, 747−754.

(5) Brown, R. A.; Spina, D.; Page, C. P. Adenosine receptors and asthma. *Br. J. Pharmacol.* **2008**, *153*, S446−456.

(6) Priego, E. M.; Perez-Perez, M. J.; von Frijtag Drabbe Kuenzel, J. K.; de Vries, H.; IJzerman, A. P.; Camarasa, M. J.; Martin-Santamaria, S. Selective human adenosine A_3 antagonists based on pyrido[2,1-*f*]purine-2,4-diones: novel features of hA_3 antagonist binding. *ChemMedChem* **2008**, *3*, 111−119.

(7) Xia, L.; Burger, W. A. C.; van Veldhoven, J. P. D.; Kuiper, B. J.; van Duijl, T. T.; Lenselink, E. B.; Paasman, E.; Heitman, L. H.; IJzerman, A. P. Structure-affinity relationships and structure-kinetics relationships of pyrido[2,1-*f*]purine-2,4-dione derivatives as human adenosine A_3 receptor antagonists. *J. Med. Chem.* **2017**, *60*, 7555−7568.

(8) Priego, E. M.; Kuenzel, J. V.; IJzerman, A. P.; Camarasa, M. J.; Perez-Perez, M. J. Pyrido[2,1-*f*]purine-2,4-dione derivatives as a novel class of highly potent human A_3 adenosine receptor antagonists. *J. Med. Chem.* **2002**, *45*, 3337−3344.

(9) Weichert, D.; Gmeiner, P. Covalent molecular probes for class A G protein-coupled receptors: advances and applications. *ACS Chem. Biol.* **2015**, *10*, 1376−1386.

(10) Murrison, E. M.; Goodson, S. J.; Edbrooke, M. R.; Harris, C. A. Cloning and characterisation of the human adenosine A_3 receptor gene. *FEBS Lett.* **1996**, *384*, 243−246.

(11) Glukhova, A.; Thal, D. M.; Nguyen, A. T.; Vecchio, E. A.; Jorg, M.; Scammells, P. J.; May, L. T.; Sexton, P. M.; Christopoulos, A. Structure of the adenosine A_1 receptor reveals the basis for subtype selectivity. *Cell* **2017**, *168*, 867−877.

(12) Li, A. H.; Chang, L.; Ji, X. D.; Melman, N.; Jacobson, K. A. Functionalized congeners of 1,4-dihydropyridines as antagonist molecular probes for A_3 adenosine receptors. *Bioconjugate Chem.* **1999**, *10*, 667−677.

(13) Baraldi, P. G.; Cacciari, B.; Moro, S.; Romagnoli, R.; Ji, X. D.; Jacobson, K. A.; Gessi, S.; Borea, P. A.; Spalluto, G. Fluorosulfonyl- and bis-(beta-chloroethyl)amino-phenylamino functionalized pyrazolo[4,3-e]1,2,4-triazolo[1,5-c]pyrimidine derivatives: irreversible antagonists at the human A_3 adenosine receptor and molecular modeling studies. *J. Med. Chem.* **2001**, *44*, 2735−2742.

(14) Ji, X. D.; Gallorodriguez, C.; Jacobson, K. A. A selective agonist affinity label for A_3 adenosine receptors. *Biochem. Biophys. Res. Commun.* **1994**, *203*, 570−576.

(15) Yang, X.; Michiels, T. J. M.; de Jong, C.; Soethoudt, M.; Dekker, N.; Gordon, E.; van der Stelt, M.; Heitman, L. H.; van der Es, D.; IJzerman, A. P. An affinity-based probe for the human adenosine A_{2A} receptor. *J. Med. Chem.* **2018**, *61*, 7892−7901.

DOI: 10.1021/acs.jmedchem.8b02026
J. Med. Chem. 2019, 62, 3539−3552

(16) Picone, R. P.; Fournier, D. J.; Makriyannis, A. Ligand based structural studies of the CB_1 cannabinoid receptor. *J. Pept. Res.* **2002**, *60*, 348−356.
(17) Narayanan, A.; Jones, L. H. Sulfonyl fluorides as privileged warheads in chemical biology. *Chem. Sci.* **2015**, *6*, 2650−2659.
(18) Grimster, N. P.; Connelly, S.; Baranczak, A.; Dong, J. J.; Krasnova, L. B.; Sharpless, K. B.; Powers, E. T.; Wilson, I. A.; Kelly, J. W. Aromatic sulfonyl fluorides covalently kinetically stabilize transthyretin to prevent amyloidogenesis while affording a fluorescent conjugate. *J. Am. Chem. Soc.* **2013**, *135*, 5656−5668.
(19) Müller, C. E.; Diekmann, M.; Thorand, M.; Ozola, V. [^{3}H]8-Ethyl-4-methyl-2-phenyl-(8R)-4,5,7,8-tetrahydro-1H-imidazo[2,1-*f*]-purin-5-one ([^{3}H]PSB-11), a novel high-affinity antagonist radioligand for human A_3 adenosine receptors. *Bioorg. Med. Chem. Lett.* **2002**, *12*, 501−503.
(20) Weichert, D.; Kruse, A. C.; Manglik, A.; Hiller, C.; Zhang, C.; Hubner, H.; Kobilka, B. K.; Gmeiner, P. Covalent agonists for studying G protein-coupled receptor activation. *Proc. Natl. Acad. Sci. U.S.A.* **2014**, *111*, 10744−10748.
(21) Yang, X.; Dong, G.; Michiels, T. J. M.; Lenselink, E. B.; Heitman, L.; Louvel, J.; IJzerman, A. P. A covalent antagonist for the human adenosine A_{2A} receptor. *Purinergic Signalling* **2017**, *13*, 191−201.
(22) Motulsky, H. J.; Mahan, L. C. The kinetics of competitive radioligand binding predicted by the law of mass-action. *Mol. Pharmacol.* **1984**, *25*, 1−9.
(23) Doornbos, M. L. J.; Wang, X.; Vermond, S. C.; Peeters, L.; Perez-Benito, L.; Trabanco, A. A.; Lavreysen, H.; Cid, J. M.; Heitman, L. H.; Tresadern, G.; IJzerman, A. P. Covalent allosteric probe for the metabotropic glutamate receptor 2: design, synthesis, and pharmacological characterization. *J. Med. Chem.* **2018**, 223−233.
(24) Jörg, M.; Glukhova, A.; Abdul-Ridha, A.; Vecchio, E. A.; Nguyen, A. T. N.; Sexton, P. M.; White, P. J.; May, L. T.; Christopoulos, A.; Scammells, P. J. Novel irreversible agonists acting at the A_1 adenosine receptor. *J. Med. Chem.* **2016**, *59*, 11182−11194.
(25) van Muijlwijk-Koezen, J. E.; Timmerman, H.; van der Sluis, R. P.; van de Stolpe, A. C.; Menge, W. M. P. B.; Beukers, M. W.; van der Graaf, P. H.; de Groote, M.; IJzerman, A. P. Synthesis and use of FSCPX, an irreversible adenosine A_1 antagonist, as a 'receptor knock-down' tool. *Bioorg. Med. Chem. Lett.* **2001**, *11*, 815−818.
(26) Strange, P. G. Use of the GTP gamma S ([^{35}S]GTP gamma S and Eu-GTP gamma S) binding assay for analysis of ligand potency and efficacy at G protein-coupled receptors. *Br. J. Pharmacol.* **2010**, *161*, 1238−1249.
(27) Liu, W.; Chun, E.; Thompson, A. A.; Chubukov, P.; Xu, F.; Katritch, V.; Han, G. W.; Roth, C. B.; Heitman, L. H.; IJzerman, A. P.; Cherezov, V.; Stevens, R. C. Structural basis for allosteric regulation of GPCRs by sodium ions. *Science* **2012**, *337*, 232−236.
(28) Picone, R. P.; Khanolkar, A. D.; Xu, W.; Ayotte, L. A.; Thakur, G. A.; Hurst, D. P.; Abood, M. E.; Reggio, P. H.; Fournier, D. J.; Makriyannis, A. (-)-7′-Isothiocyanato-11-hydroxy-1 ‘,1′-dimethylheptylhexahydrocannabinol (AM841), a high-affinity electrophilic ligand, interacts covalently with a cysteine in helix six and activates the CB1 cannabinoid receptor. *Mol. Pharmacol.* **2005**, *68*, 1623−1635.
(29) Singh, J.; Petter, R. C.; Baillie, T. A.; Whitty, A. The resurgence of covalent drugs. *Nat. Rev. Drug Discovery* **2011**, *10*, 307−317.
(30) Soethoudt, M.; Stolze, S. C.; Westphal, M. V.; van Stralen, L.; Martella, A.; van Rooden, E. J.; Guba, W.; Varga, Z. V.; Deng, H.; van Kasteren, S. I.; Grether, U.; IJzerman, A. P.; Pacher, P.; Carreira, E. M.; Overkleeft, H. S.; Ioan-Facsinay, A.; Heitman, L. H.; van der Stelt, M. Selective photoaffinity probe that enables assessment of cannabinoid CB_2 receptor expression and ligand engagement in human cells. *J. Am. Chem. Soc.* **2018**, *140*, 6067−6075.
(31) Goebel, U.; Siepe, M.; Schwer, C.; Schlensak, C.; Loop, T. Sevoflurane-induced preconditioning in the isolated mouse heart is mediated by A_1-and A_3-adenosine receptors. *Eur. J. Anaesthesiol.* **2010**, *27*, 72.
(32) Sherman, W.; Day, T.; Jacobson, M. P.; Friesner, R. A.; Farid, R. Novel procedure for modeling ligand/receptor induced fit effects. *J. Med. Chem.* **2006**, *49*, 534−553.
(33) Heitman, L. H.; Göblyös, A.; Zweemer, A. M.; Bakker, R.; Mulder-Krieger, T.; van Veldhoven, J. P. D.; de Vries, H.; Brussee, J.; IJzerman, A. P. A series of 2,4-disubstituted quinolines as a new class of allosteric enhancers of the adenosine A_3 receptor. *J. Med. Chem.* **2009**, *52*, 926−931.
(34) Smith, P. K.; Krohn, R. I.; Hermanson, G. T.; Mallia, A. K.; Gartner, F. H.; Provenzano, M. D.; Fujimoto, E. K.; Goeke, N. M.; Olson, B. J.; Klenk, D. C. Measurement of protein using bicinchoninic acid. *Anal. Biochem.* **1985**, *150*, 76−85.
(35) Boussif, O.; Lezoualch, F.; Zanta, M. A.; Mergny, M. D.; Scherman, D.; Demeneix, B.; Behr, J. P. A versatile vector for gene and oligonucleotide transfer into cells in culture and in-vivo - polyethylenimine. *Proc. Natl. Acad. Sci. U.S.A.* **1995**, *92*, 7297−7301.
(36) Gorman, C. M.; Howard, B. H.; Reeves, R. Expression of recombinant plasmids in mammalian-cells is enhanced by sodium-butyrate. *Nucleic Acids Res.* **1983**, *11*, 7631−7648.
(37) Yung-Chi, C.; Prusoff, W. H. Relationship between the inhibition constant (K_I) and the concentration of inhibitor which causes 50 per cent inhibition (I_{50}) of an enzymatic reaction. *Biochem. Pharmacol.* **1973**, *22*, 3099−3108.

DOI: 10.1021/acs.jmedchem.8b02026
J. Med. Chem. 2019, 62, 3539−3552